The electrical resistivity structure of Archean to Tertiary lithosphere along 3200 km of SNORCLE profiles, northwestern Canada[1, 2]

Alan G. Jones, Juanjo Ledo, Ian J. Ferguson, Colin Farquharson, Xavier Garcia, Nick Grant, Gary McNeice, Brian Roberts, Jessica Spratt, Grant Wennberg, Lisa Wolynec, and Xianghong Wu

Abstract: Magnetotelluric (MT) measurements to image the three-dimensional resistivity structure of the North American continent from an Archean core to a region of Tertiary assembly were recorded at almost 300 sites along 3200 km of profiles on the Lithoprobe Slave – Northern Cordillera Lithospheric Evolution (SNORCLE) transect in northwestern Canada. At the largest scale, the MT results indicate significant lithospheric thickness variation, from 260 km at the southwest margin of the Slave craton to significantly < 100 km at the southwestern end of the SNORCLE transect in the Cordillera. At intermediate scale, the resistivity results allow broad terrane subdivisions to be made. Several anomalously conductive zones along the SNORCLE transect, in rocks ranging in age from Archean to Tertiary, are attributed to the introduction of either water or carbon into the crust and mantle during subduction processes. At the local scale, the MT data image two major faults crossing the study area, the Great Slave Lake shear zone and the Tintina Fault. The resistivity images show that both the Tintina Fault and Great Slave Lake shear zone form crustal-scale features, and that the Tintina Fault has a remarkably uniform resistivity signature over a 400 km strike length in the study area. Arguably the most controversial conclusion reached is that the MT data do not support the western extension of North American autochthonous basement suggested from interpretation of the seismic reflection data.

Résumé : Afin d'obtenir une image de la structure de résistivité en trois dimensions du continent nord-américain, d'un noyau archéen à une région d'assemblage tertiaire, des mesures magnétotelluriques (MT) ont été enregistrées à près de 300 sites le long de 3200 km de profils de la géotraverse SNORCLE du projet Lithoprobe dans le nord-ouest du Canada. À la plus grande échelle, les résultats magnétotelluriques indiquent des variations importantes d'épaisseur de la lithosphère, de 260 km à la bordure sud-ouest du craton des Esclaves à passablement moins de 100 km à l'extrémité sud-ouest de la géotraverse SNORCLE, dans la Cordillère. À une échelle intermédiaire, les résultats des données de résistivité permettent de subdiviser le terrain en de larges terranes. Plusieurs anomalies de zones conductrices le long de la géotraverse SNORCLE, dans des roches datant de l'Archéen au Tertiaire, sont attribuées à l'introduction de carbone ou d'eau dans la croûte et le manteau durant les processus de subduction. À une échelle locale, deux failles majeures traversent la région à l'étude, la zone de cisaillement du Grand lac des Esclaves et la faille Tintina. Les images de résistivité montrent que la faille Tintina et la zone de cisaillement du Grand lac des Esclaves sont des éléments d'une échelle crustale et que la faille Tintina a une signature de résistivité remarquablement uniforme sur une longueur de 400 km, selon la direction, dans la région à l'étude. Tel que suggéré par l'interprétation des données de sismique réflexion, il est permis de croire que la conclusion la plus controversée est que les données MT ne supportent pas l'extension vers

Received 22 June 2004. Accepted 13 July 2005. Published on the NRC Research Press Web site at http://cjes.nrc.ca on 26 September 2005.

Paper handled by Associate Editor R.M. Clowes.

A.G. Jones,[3, 4] J. Ledo,[5] X. Garcia,[4] N. Grant, B. Roberts, and J. Spratt.[4] Geological Survey of Canada, 615 Booth St., Ottawa, ON K4M 1E3, Canada.
I.J. Ferguson, G. Wennberg, L. Wolynec, and X. Wu. Department of Geological Sciences, University of Manitoba, Winnipeg, MN R3T 2N2, Canada.
C. Farquharson. Department of Earth and Ocean Sciences, The University of British Columbia, 6339 Stores Road, Vancouver, BC V6T 1Z4, Canada.
G. McNeice.[6] Phoenix Geophysics Ltd., 3781 Victoria Park Avenue, Unit #3, Scarborough, ON M1W 3K5, Canada.

[1]This article is one of a selection of papers published in this Special Issue on *The Lithoprobe Slave – Northern Cordillera Lithospheric Evolution (SNORCLE) transect*.
[2]Lithoprobe Publication 1408. Dublin Institute for Advanced Studies Publication GP174.
[3]Corresponding author (e-mail: alan@cp.dias.ie).
[4]Present address: Dublin Institute for Advanced Studies, 5 Merrion Square, Dublin 2, Ireland.
[5]Present address: Dept. Geodinamica i Geofisica, Facultat de Geologia, c/ Marti i Franques, s/n 08028 Barcelona, Spain.
[6]Present address: Geosystem Canada Ltd., 927 Raftsman Lane, Ottawa, ON K1C 2V3, Canada.

 doi: 10.1139/E05-080 © 2005 NRC Canada

l'ouest du socle autochtone de l'Amérique du Nord.

[Traduit par la Rédaction]

Introduction

The Lithoprobe Slave-NORthern Cordillera Lithospheric Evolution (SNORCLE) transect records, in a compact area unique in the world, the results of geological processes dating from the Archean to the Tertiary. The transect traverses, from east to west, the Archean Slave craton, the Paleoproterozoic Wopmay orogen, adjacent Neoproterozoic rocks, and finally the Proterozoic to Tertiary rocks of the northern Canadian Cordillera. As part of Lithoprobe, and related, investigations lithosphere-probing magnetotelluric (MT) soundings have been made at a total of almost 300 sites along 3200 km of profiles on the SNORCLE transect. The MT soundings were made along the three main SNORCLE corridors, corridors 1 and 1A, 2, and 3 (Fig. 1), with additional recordings in the Slave craton (profile 1S in Fig. 1 plus other locations), and on two shorter profiles in the Cordillera (profiles 4 and 5 in Fig. 1). The general objectives established for the electromagnetic studies on the SNORCLE transect included characterization of regional resistivity properties, delineation of the sub-surface geometry of major faults, and determination of the depth to the base of the lithosphere (Clowes 1993, 1997).

Broadband and long-period MT surveys provide images and models of the electrical resistivity structure of the crust and upper mantle, and the geometries obtained allow inferences to be made about the tectonic structure and history of a region. Electrical resistivity is sensitive to a variety of geological parameters, e.g., the presence of interconnected graphite, metallic oxides, sulphides, and aqueous fluids in the crust; and graphite, grain-boundary carbon, hydrated minerals, aqueous fluids, partial melt, and oxygen fugacity in the mantle. These are, in the main, minor constituents of a rock matrix in fraction, but have significant influence on physical state and rheological properties, and thus provide information that is complementary to that from other geophysical methods that are predominantly bulk properties. The natural-source MT method is an attractive electromagnetic method for regional studies for a variety of reasons, especially its ease of operation logistically and its assured penetration to all depths. Recent reviews of continental crustal and lithospheric mantle MT work can be found in Jones (1998, 1999), Heinson (1999), and Jones and Craven (2004).

In this paper, we focus on a new synthesis of MT results from the SNORCLE transect. Maps of MT responses are presented to examine the large-scale changes in crust and mantle resistivity between different regions and between lithosphere of different ages. The variation in the anisotropy of the MT response is also examined: this parameter provides a measure of the degree of structural complexity in different regions. Finally, the MT data from corridors 1 and 2 are used to produce a regional-scale resistivity model of the whole transect, representing the characterization of lithosphere ranging in age from the Archean to the Tertiary. Information on the crust and mantle lithosphere is extracted from this model, and its comparison with a more detailed model of the corridor 3 data.

Descriptions of the processing of the SNORCLE MT data set have been presented elsewhere: Wu (2001) and Jones and Spratt (2002) describe extraction of impedance responses from MT data collected at auroral and sub-auroral latitudes, and Wennberg (2003) and Ledo et al. (2004) describes detailed MT tensor decompositions for the data along corridors 2 and 3 respectively. Detailed modelling and inversion, and geological interpretation of individual segments of the MT data, have also been completed. Results from the centre of the Slave craton are described in Jones et al. (2001, 2003) and compared with the western Superior craton in Jones and Craven (2004). Results for the Yellowknife Fault Zone and surrounding region are described in Jones and Garcia (2005), and results for the Anton complex in Jones and Ferguson (2001). Results from the Wopmay orogen are described in Wu et al. (2005), and earlier electromagnetic soundings in the north of this orogen are described by Camfield et al. (1989). The resistivity structure along corridor 3 in the Cordillera is described by Wolynec (2000) and Ledo et al. (2004), and along corridor 2 by Wennberg et al. (2002). Wu et al. (2002) use the MT data to image the Great Slave Lake shear zone, and Ledo et al. (2002) use the MT data to image the Tintina Fault. Finally, Eaton et al. (2004) compare and contrast the seismic and electrical anisotropy across the Great Slave Lake shear zone.

Tectonic setting and objectives of electromagnetic surveys

Slave craton

The eastern end of SNORCLE transect corridor 1 traverses the southwestern part of the Archean Slave craton (Fig. 1). The Slave craton includes gneissic to massive granitoid rocks including gneissic basement (> 3.1 Ga), younger granitic plutons (2.7–2.6 Ga), and interspersed turbidite-volcanic assemblages (2.72–2.66 Ga). The crust of the craton was almost completely assembled by 2.69 Ga (Hoffman 1989; Davis and Bleeker 1999). Davis et al. (2003) present a tectonic scenario model for the development of the Slave lithosphere that explains all the known geological, geophysical, geochemical, petrological, and geochronological data, and the information from the MT studies provided key geometrical information in the construction of that model.

SNORCLE corridor 1 crosses the Anton complex located in the southwest of the Slave craton. This complex is now recognized as an integral part of an early to mid-Achaean basement complex, the so-called Central Slave Basement Complex (CSBC, Fig. 1), of much of the Slave craton (Bleeker et al. 1999*a*, 1999*b*), and is not a distinct Archean terrane (Kusky 1989, 1990).

The specific objectives of the MT measurements in the Slave craton were the determination of structures within the

© 2005 NRC Canada

Fig. 1. Tectonic map of northwestern Canada showing the locations of the SNORCLE corridors (red numbered lines) and the profile for the regional magnetotelluric (MT) model (black line). Individual MT station locations are shown in Figs. 4 and 5. Terranes of the Cordillera are labelled. Displaced continental margin terranes: NS, Nisling; CA, Cassier. Pericratonic terrane; KO, Kooteney. Accreted terranes: CC, Cache Creek; ST, Stikine; QN, Quesnelia; SM, Slide Mountain; DY, Dorsey. Insular superterrane: AX, Alexander; WR, Wrangelia. m, Undivided metamorphic rock. CSBC, Central Slave Basement Complex; GSLsz, Great Slave Lake shear zone.

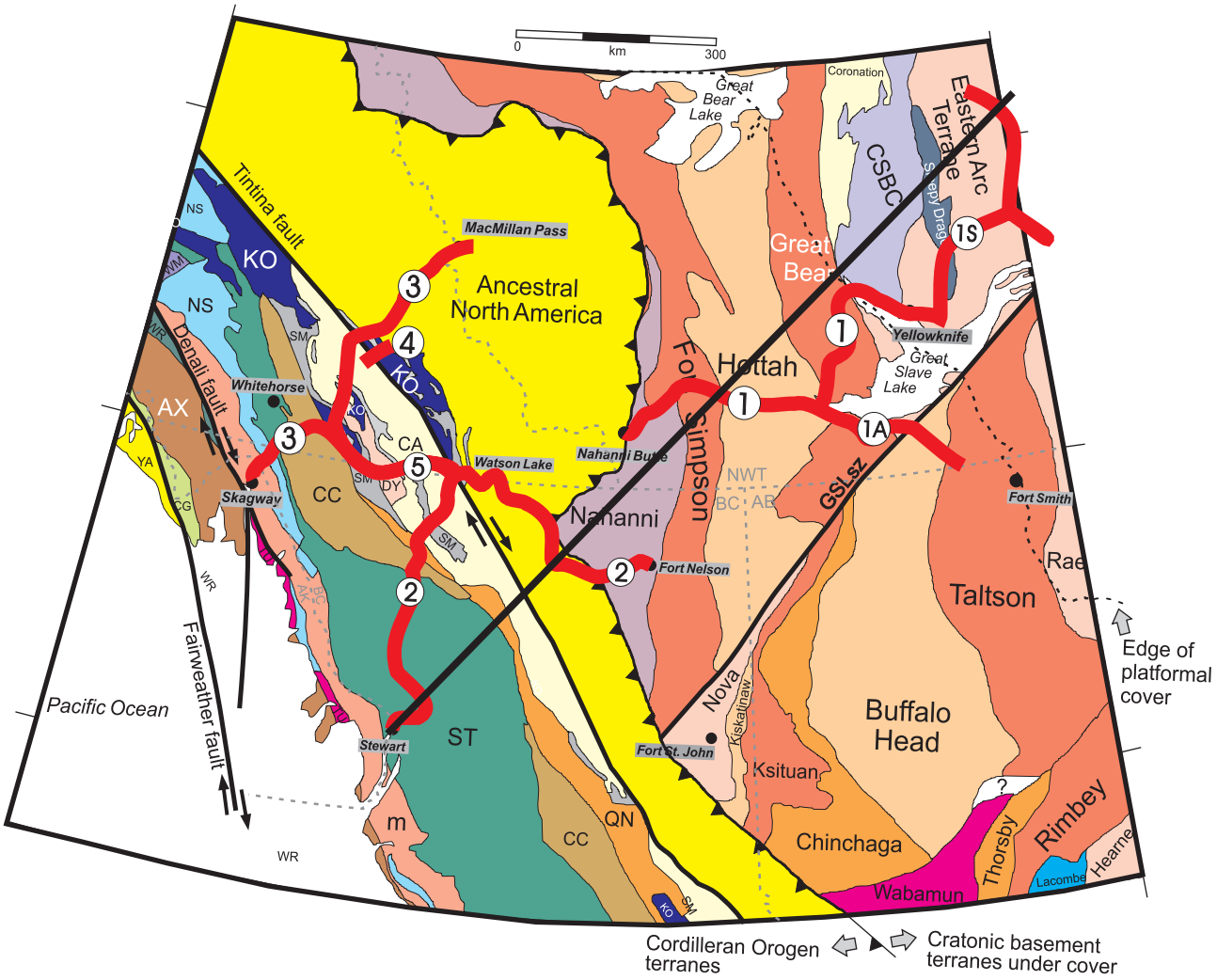

lithosphere of the craton and the depth to the lithosphere–asthenosphere boundary and its topology. The MT results serendipitously revealed an anomalous upper mantle conducting region, named the Central Slave Mantle Conductor, that is spatially collocated with the central Slave Eocene diamondiferous kimberlite field (the so-called "Corridor of Hope," Fipke et al. 1995), and spatially and in depth with a geochemically defined ultra-depleted, harzburgitic layer (Griffin et al. 1999).

Great Slave Lake shear zone

The Great Slave Lake shear zone (GSLsz) is a northeast-trending dextral continental transform fault, with up to 700 km of strike-slip motion, extending from the Rocky Mountains to the southeast side of Great Slave Lake (Hoffman 1987). It is linked to convergence and collision between the Archean craton and Rae Province in the Paleoproterozoic (Hoffman 1987; Hanmer et al. 1992). Post-collisional convergence of the Slave and Rae provinces at ca. 1800 Ma produced an additional 75–125 km of strike-slip motion on the later brittle McDonald Fault (MF), which is partially coincident with the GSLsz (Hanmer et al. 1992; Ritts and Grotzinger 1994) in the survey area.

One of the specific objectives of the SNORCLE transect investigations was to determine the geometry and lithospheric extent of the GSLsz, given its continental scale. Unfortunately, corridor 1A (Fig. 1) was deemed lowest priority for seismic reflection acquisition, so no correlative reflection data exist for comparison with the MT soundings made along corridor 1A. Fortunately, teleseismic measurements were made across the GSLsz by Eaton and Hope (2003), and the comparison between seismic and electrical anisotropy is discussed in Eaton et al. (2004).

Wopmay orogen and adjacent Paleoproterozoic terranes

The western part of corridor 1 crosses the 1.9–1.8 Ga Proterozoic Wopmay orogen, which comprises a series of north–south-trending tectonic units formed as microcontinents

© 2005 NRC Canada

and volcanic arcs that were accreted to the western margin of the Slave craton (Hildebrand et al. 1987).

The passive western margin of the Slave craton is recorded in the Coronation margin rocks exposed 200 km to the north of the Lithoprobe corridor (Hoffman and Bowring 1984). The Hottah terrane consists of magmatic arc and associated sedimentary rocks that formed to the west of the Slave Province at 1.92–1.90 Ga (Hildebrand et al. 1987). Collapse of the ocean basin off the western Slave Province occurred during the 1.90–1.86 Ga Calderan orogeny. During terminal collision some of the Hottah terrane rocks were thrust over the Coronation Supergroup rocks as both were thrust over the Slave craton (Cook et al. 1999). The 1.875–1.84 Ga Great Bear magmatic arc was deposited on both the Hottah terrane and deformed rocks of the Coronation margin, and forms a 100 km-wide zone of volcano-sedimentary sequences and plutonic rocks (Hildebrand et al. 1987). The Fort Simpson terrane contains 1.845 Ga magmatic rocks, and its terminal collision with the Hottah terrane occurred after the formation of these rocks and pre-1.710 Ga (Villeneuve et al. 1991). The Nahanni terrane is located to the west of the Fort Simpson crust. It is characterized by variable, but mostly low-magnitude, magnetic anomalies (Pilkington et al. 2000). Cook et al. (1999) suggest that the magnetic low may be associated with thinned Fort Simpson crust. However, isotopic dating of rocks, presumed to be derived from the Nahanni terrane in overlying units, has indicated younger ages, suggesting that the terrane may contain components with a different origin (Aspler et al. 2003).

Along the Lithoprobe transect, Proterozoic rocks of the Wopmay orogen are overlain by Phanerozoic sedimentary rocks. The eastern margin of the cover is in the Great Bear magmatic arc, and the thickness of the sedimentary rocks increases from east to west, reaching a value of around 1000 m over the Fort Simpson terrane. The Phanerozoic sequence is Middle to Upper Devonian in age and consists of gently westward-dipping shales, siltstones, and limestone units (Aitken 1993).

The primary objective of the MT study of the Wopmay orogen was to characterize the geoelectric structure of the Proterozoic terranes and their margins. The MT results also provide images of the Phanerozoic sedimentary rocks (Wu 2001; Wu et al. 2005).

Fort Simpson basin and Proterozoic passive margin rocks

At the western end of corridor 1 seismic reflection data have identified the presence of a thick sequence of west-dipping reflectors that define a west-facing monocline (Cook et al. 1999). These rocks were interpreted as a basin that formed within the Fort Simpson terrane during a period of lithospheric extension.

More recent interpretations incorporating Lithoprobe seismic reflection results from the eastern parts of corridors 2 and 3 suggest that the rocks in the basin may form part of an extensive sequence of passive margin sedimentary rocks (Snyder et al. 2002). Based on outcrop correlations these rocks are considered to include the 1.84–1.71 Ga Wernecke Supergroup, the 1.815–1.5 Ga Muskwa assemblage, the 1.2–0.78 Ga Mackenzie Mountain Supergroup, and the 0.8–0.54 Ga Windermere Supergroup. These rocks are interpreted to form a westward-tapering wedge (WTW) that extends through the middle to lower crust of the Cordillera upon which thin flake Cordilleran terranes were accreted (Cook et al. 2001, 2004; Snyder et al. 2002).

The SNORCLE MT data permit an examination of the resistivity character of these Proterozoic rocks. Sites at the end of the western end of corridor 1 are located above the Fort Simpson basin and sites in the eastern half of corridors 2 and 3 lie above regions in which the seismic reflection data define a substantial thickness of Proterozoic rocks in the middle and lower crust. The resolution of the Proterozoic rocks by the MT results is restricted by the overlying thick Phanerozoic sediments at the western end of corridor 1 (Aitken 1993) and by the overlying Cambrian to Devonian rocks of the Selwyn basin at the eastern end of corridor 3 (Gordey and Anderson 1993).

Northern Cordillera

The Cordillera of western Canada consists of a collage of pre-Cordilleran sediments, oceanic and island-arc terranes (accreted since the Neoproterozoic), and igneous rocks, with most of the westward growth occurring during the Mesozoic. In northern Canada, the tectonic elements have since been displaced northward along large dextral strike-slip faults due to the relative motion between the Pacific Ocean basin and the North American continent. Broadly, the Canadian Cordillera can be divided into five major morphogeological and physiographic fault-bounded belts (Gabrielse and Yorath 1991), which are, from west to east, the Insular Belt, the Coast Belt, the Intermontane Belt, the Omineca Belt, and the Foreland Belt. Their development reflects Mesozoic and Cenozoic collision and deformation along the northwestern margin of North America. Of these, the SNORCLE MT surveys included sites crossing the cordillera from the Coast Belt to the Foreland Belt.

The SNORCLE MT investigations in the cordillera had three principal objectives. The primary objective is the characterization of the regional conductivity properties of the northern Cordillera in relation to the major tectonic units, the second thrust involves imaging upper mantle features, and the third specific goal is the determination of the subsurface geometry and character of the Tintina strike-slip fault zone.

Data acquired

Magnetotelluric data were acquired on the SNORCLE transect as part of Lithoprobe studies, with additional commercial support, and other studies funded by the National Science Foundation and the Geological Survey of Canada (GSC). Table 1 lists the surveys undertaken, locales, instrumentation used, and the numbers of sites.

The instrumentation was basically of two types, broadband MT (BBMT) systems, which recorded data in the frequency range of typically 1000–0.001 Hz (1000 s), and long-period MT (LMT) systems, which recorded data in the frequency range of 0.05–0.0001 Hz (20 – 10 000 s). BBMT acquisition typically required 2–3 nights of recording, whereas LMT acquisition required 3–4 weeks, at each location. There were three types of BBMT systems used. The first Phoenix survey, in 1996, used their 16-bit V5 system, whereas the later Phoenix surveys used their 24-bit V5-2000 system. The 1998

© 2005 NRC Canada

Table 1. Magnetotelluric surveys undertaken as part of the SNORCLE transect investigations.

Year and type	Funding	Locale	Instrumentation	No. of stations
1996	Lithoprobe	Corridors 1 and 1A	Phoenix V5	BBMT: 60
Land-based	GSC		GSC LiMS	LMT: 56
1998	Lithoprobe	Southern part of winter road	Phoenix V5-2000	BBMT: 12
Winter road	DeBeers		GSC LiMS	LMT: 11
	Kennecott			
	GSC			
1999	Lithoprobe	Central and northern parts of winter road	Phoenix V5-2000	BBMT: 19
Winter road	DeBeers		GSC LiMS	LMT: 18
	Kennecott			
	GSC			
1999	Lithoprobe	Corridors 2, 2A, and 3	Metronix ADU-06	BBMT: 151
Land-based	GSC		GSC LiMS	LMT: 75
2000	Lithoprobe	Southern part of winter road	Metronix ADU-06	BBMT: 12
Winter road	DeBeers			LMT: 12
	Kennecott			
	GSC			
2000	GSC	Around Yellowknife	Metronix ADU-06	BBMT: 8
Frozen lakes	(EXTECH-III)			
1999–2000	NSF	Slave craton	WHOI ocean bottom systems	LMT: 10
Lakes	Lithoprobe			
2000–2001	NSF Lithoprobe	Slave craton	WHOI ocean bottom systems	LMT: 9
Lakes				
2000	GSC	Eastern Slave	GSC LiMS	LMT: 15
Land-based	(TGI)			

winter road survey, in March of that year, was the first commercial survey undertaken with the-then brand new V5-2000 systems. The final BBMT surveys, let to Geosystem Canada, used Metronix ADU-06 MT systems but with EMI coil magnetometers. The LMT measurements used the GSC-designed long-period MT systems (LiMS, Andersen et al. 1988), with ring-core fluxgate magnetometers (Narod and Bennest 1990).

The first survey, in 1996, was a commercial survey let to Phoenix Geophysics Ltd. (Toronto, Ontario) for acquisition of BBMT data at 60 sites along SNORCLE corridors 1 and 1A (Fig. 1). In addition, LMT measurements were made at 56 of the BBMT locations.

Subsequently, using Lithoprobe and industry funds MT surveys took place on the winter roads of the Slave craton during March of 1998, 1999, and 2000 (corridor 1S in Fig. 1). These surveys required novel acquisition of electric fields by lowering the electrodes to the bottoms of lakes through holes drilled through the ice, and acquisition of the magnetic fields on the shores of the lakes. Prior tests had demonstrated that the lake ice moves with periodicities in the 10–100 s band, and those movements introduce high noise levels on the coil magnetometers (McNeice and Jones 1998). Fortunately, the new V5-2000 systems permitted acquisition of the electric field data at a location apart from the magnetic field data.

A second novel experimental component specific to the Slave craton involved deploying electromagnetic (EM) instrumentation designed for ocean-bottom MT acquisition. These instruments, from Woods Hole Oceanographic Institution, were constructed for deployment on the continental shelves (Petitt et al. 1994), and were first used in the Southern Appalachians MT project (Ogawa et al. 1996; Wannamaker et al. 1996). The 10 instruments were deployed in 1999 from a float plane by a specially designed winch constructed for us by Air Tindi. They were deployed during August when the lakes were ice-free, and recovered the following July (2000). They were then re-deployed at nine new locations (one instrument could not be re-deployed) in August 2000, and re-recovered in July 2001.

The final MT experiment on the Slave craton was funded through the Canadian Federal Government's Targeted Geoscience Initiative (TGI) and comprised two profiles, of LMT systems only, in the eastern part of the craton. The systems were installed with float plane and helicopter support.

In the Autumn of 1999, the largest contract MT survey let by Lithoprobe was undertaken by Geosystem-Canada and comprised 151 BBMT sites along SNORCLE corridors 2 and 3 (Fig. 1), plus a connection between the two corridors corridor 5) and an additional short line across the Tintina Fault (corridor 4, Fig. 1). In addition, GSC and University of Manitoba students made LMT measurements at 75 of those locations, essentially at every second BBMT site.

Electrical parameter maps

Depth transformation

From the MT data acquired at the locations shown in Fig. 1 maps can be constructed of various electrical parameters for various depths. The approximate depth transformation

© 2005 NRC Canada

Fig. 2. One-dimensional resistivity-depth model of the Earth and the Niblett–Bostick transformation of the synthetic data generated from it.

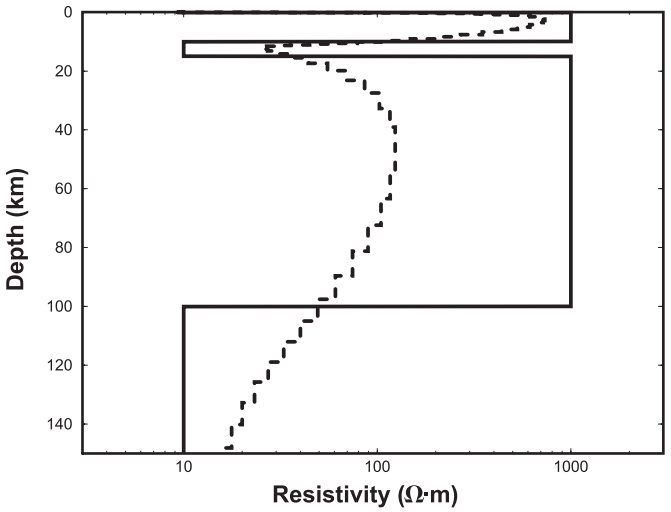

used is the so-called Niblett–Bostick (N–B) transform (Niblett and Sayn-Wittgenstein 1960; Bostick 1977; Jones 1983). This transform takes the apparent resistivity and phase data as a function of period and converts it to approximate depth by

$$\rho_{\mathrm{NB}}(h_{\mathrm{NB}}) = \rho_a(T)\left(\frac{\pi}{2\phi(T)} - 1\right)$$

and

$$h_{\mathrm{NB}} = \sqrt{\frac{\rho_a(T)\,T}{2\pi\mu_0}}$$

where T, $\rho_a(T)$ and $\varphi(T)$ are the data, namely the apparent resistivity and phase at period T, and ρ_{NB} and h_{NB} are the transformed data, namely the N–B resistivity at depth h_{NB}. It should be appreciated that this is an approximate transformation from period to depth, it is not a formal inversion. An example of the depth transformation is shown in Fig. 2. The solid line is the true layered-Earth model, whereas the dashed line is the N–B transform of synthetic data generated from the true model. Less resistive (i.e., conductive) regions are easily identified by the N–B transform, but the resistivity of resistive regions is typically underestimated. This is however a general problem of the "masking" effect in MT data whereby the parameters of a resistive region below a conductive one are difficult to determine (see, e.g., Jones 1999).

Analogously to seismic shear-wave splitting SKS plots, authors have recently chosen to display MT strike information as maps of strike arrows, but with the difference that the arrows are for specific periods, thought to be analogous to depth penetration (e.g., Jones and Gough 1995; Simpson 2001; Bahr and Simpson 2002). However, unlike seismic parameters that vary laterally by a few percent, electrical resistivity varies by many orders of magnitude, and this has a dramatic effect on penetration. In particular, for a two-dimensional (2-D) Earth the two modes of propagation, TE (transverse-electric, currents travelling along strike) and TM (transverse-magnetic, currents travelling perpendicular to strike), can penetrate to different depths at the same period. As an example Fig. 3A shows the MT responses observed at a location directly on top of the North American Central Plains (NACP) conductivity anomaly (Jones and Craven 1990; Jones et al. 1993). The NACP anomaly is virtually invisible to the TM-mode data (open circles), whereas the anomaly has a major effect on the TE-mode (filled circles) responses (Jones 1993; Fig. 3).

The N–B transformation of these data from period into approximate depth yields the data shown in Fig. 3B. As is apparent in the original data, the TM-mode EM fields do not sense the presence of the crustal NACP anomaly as it is thin laterally, so the TM-mode fields penetrate quickly through the crust into the underlying mantle (Jones 1993). At 1000 and 3000 s periods the TM-mode data are penetrating to depths of ~50 and 100 km, respectively. In contrast, the TE-mode EM fields are highly affected by the presence of the crustal conductor and become arrested in it when the penetration depth is >~12 km. The 1000 and 3000 s TE-mode data (both apparent resistivities and phases) are only penetrating to depths of 17 and 30 km, respectively.

This effect, analogous to polarizing glasses, raises a significant caution about geoelectric strike directions presented for a single long period (Jones 2002). Clearly, inferences formed from periods of 1000 or 3000 s averages together information from different depths for the two different modes of propagation. To determine the geoelectric anisotropy information, i.e., strike direction and magnitude of anisotropy (usually given by the difference on the two phase values), the data must first be transformed to the depth domain. For these data, the 300 s TM data should be compared with the 1000 s TE data, and the 500 s TM data with the 3000 s TE data. The longer period TM data (> 500 s) have no TE equivalents. This problem is evident in regional interpretations, and as an example Korja et al. (2003) recently demonstrated that supposed lithospheric anisotropy deduced from long period geoelectric strikes by Bahr and Simpson (2002) can be explained in terms of crustal heterogeneity. To try to minimize such issues, the MT data are not plotted in terms of period, but are transformed to approximate depth, using the N–B transform, prior to the averages being formed.

Electrical parameters

Maps of the following electrical parameters were generated from the MT database:

(1) Averaged resistivity: The averaged resistivity at a given N–B depth was determined from the arithmetic mean of the two impedances in the two orthogonal directions, this is the so-called Berdichevsky average (Berdichevsky and Dmitriev 1976). This resistivity is rotationally invariant, i.e., independent of direction.

(2) Maximum and minimum resistivities: These resistivities were determined by rotating the Zxy impedance tensor element through 180°, undertaking an N–B transform at each direction, and determining the maximum and minimum resistivities for a given N–B depth. These resistivities are dependent on direction.

(3) Anisotropy: The anisotropy at a given depth was derived from taking the maximum resistivity, and the resistivity in the direction 90° from it, and computing the anisotropy percentage as

© 2005 NRC Canada

Fig. 3. (A) MT data, plotted in conventional log(period) format, from above the North American Central Plains conductivity anomaly showing the large difference in response between the along-strike currents (TE-mode, full circles) and the across-strike currents. Data at 300, 1000, and 3000 s are highlighted using the alternate colour. (B) The same data after Niblett–Bostick transformation into approximate depth. Data for the two modes have dramatically different depth sensitivity, with the TE-mode responses stalled in the crust due to the presence of the crustal conductors.

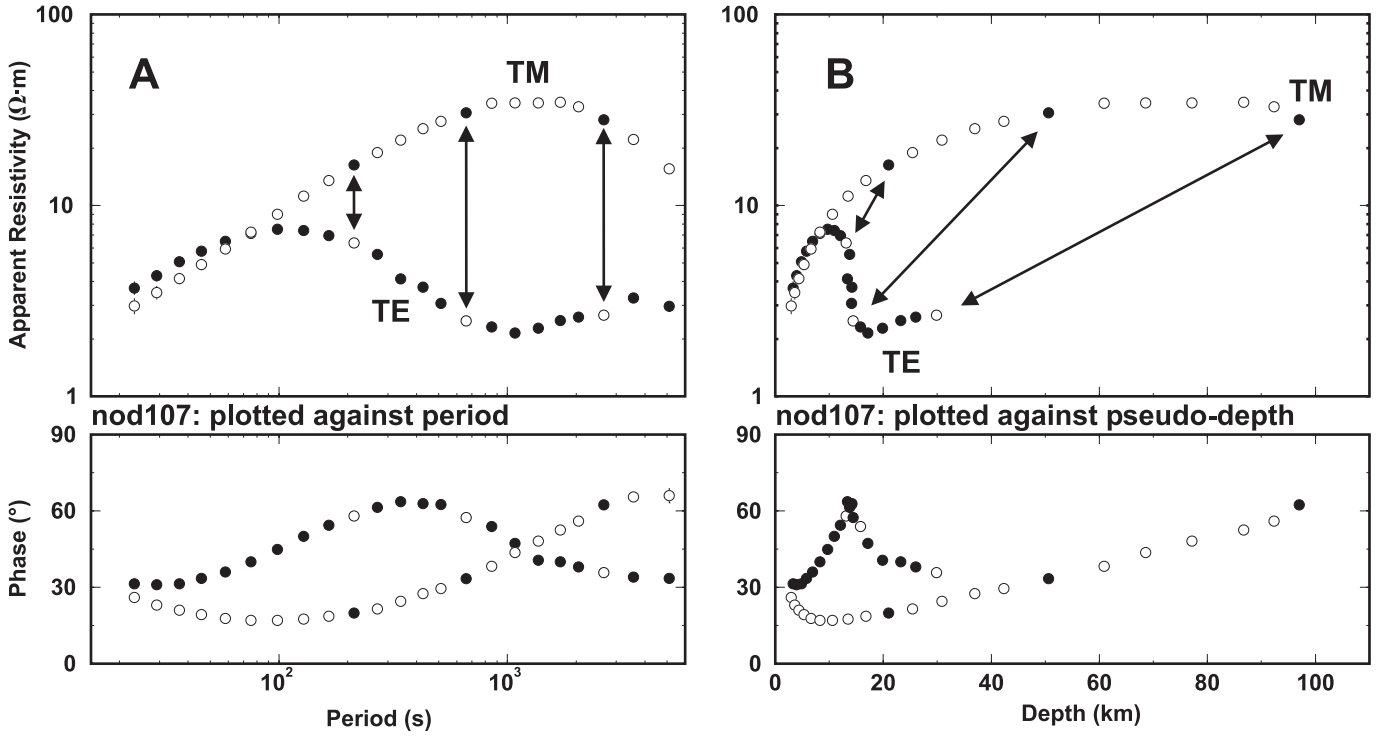

$$\text{anisotropy } (\%) = \frac{\log\left(\rho_{NB}(h,\ \Theta_{max})\right) - \log\left(\rho_{NB}(h,\ \Theta_{max}+90)\right)}{\log\left(\rho_{NB}(h,\ \Theta_{max})\right)} \times 100$$

Note that this anisotropy is electrical anisotropy and cannot be interpreted in terms of either macro, i.e., structural, or micro, i.e., grain boundary, anisotropy. Other information must be used to distinguish between these two.

Maps of the averaged resistivities and the percentage anisotropy are shown and discussed in the following section. Note that static shift effects (Jones 1988) are not treated explicitly, but the spatial smoothing described later in the text removes anomalous single site problems. Systematic shifts at a number of sites within a region are not, sensu stricto, static shifts but are due to resistivity structures that should be interpreted.

Map construction

The maps were constructed using Wessel and Smith's (1991) Generic Mapping Tools (GMT). The three steps were

(1) Spatial smoothing using median filter routine *blockmedian* with an increment of 5 min.
(2) Creating a grid from the smoothed data using a nearest neighbour algorithm *nearneighbor* with a 5 min grid spacing and a 3° search radius.
(3) Plotting, using *gridimage*.

Average resistivity maps

Maps of the averaged resistivity at depths of 5 km (middle of upper crust), 20 km (middle of the crust), 40 km (approximate base of the crust), and 100 km (middle to base of the lithosphere) are shown in Figs. 4. The black squares show the MT sites used to derive the maps. The sites used vary from map to map; some sites do not have sufficiently short period information, such as from the WHOI lakes sites or the 2000 TGI survey, whereas others do not have data at sufficiently long periods.

The immediate first-order observation from Figs. 4 is the dramatic difference in crustal resistivity between the Archean Slave craton and the terranes of the Cordillera. This is especially evident in the 5 km depth map (Fig. 4A), but also can be seen in the 20 km and 40 km depth maps (Figs. 4B, 4C). Other observations are as follows:

(1) The lithosphere beneath the southwestern Slave and immediately adjacent Wopmay orogen is highly resistive when compared with other parts of the Slave and especially when compared with the Cordillera. This observation was noted in the earliest qualitative interpretations of Jones and Ferguson (1997), and in the modelling of Jones et al. (2001, 2003), and Jones and Garcia (2005).

© 2005 NRC Canada

Fig. 4. Maps of the averaged resistivity at depths of (A) 5 km, (B) 20 km, (C) 40 km, and (D) 100 km.

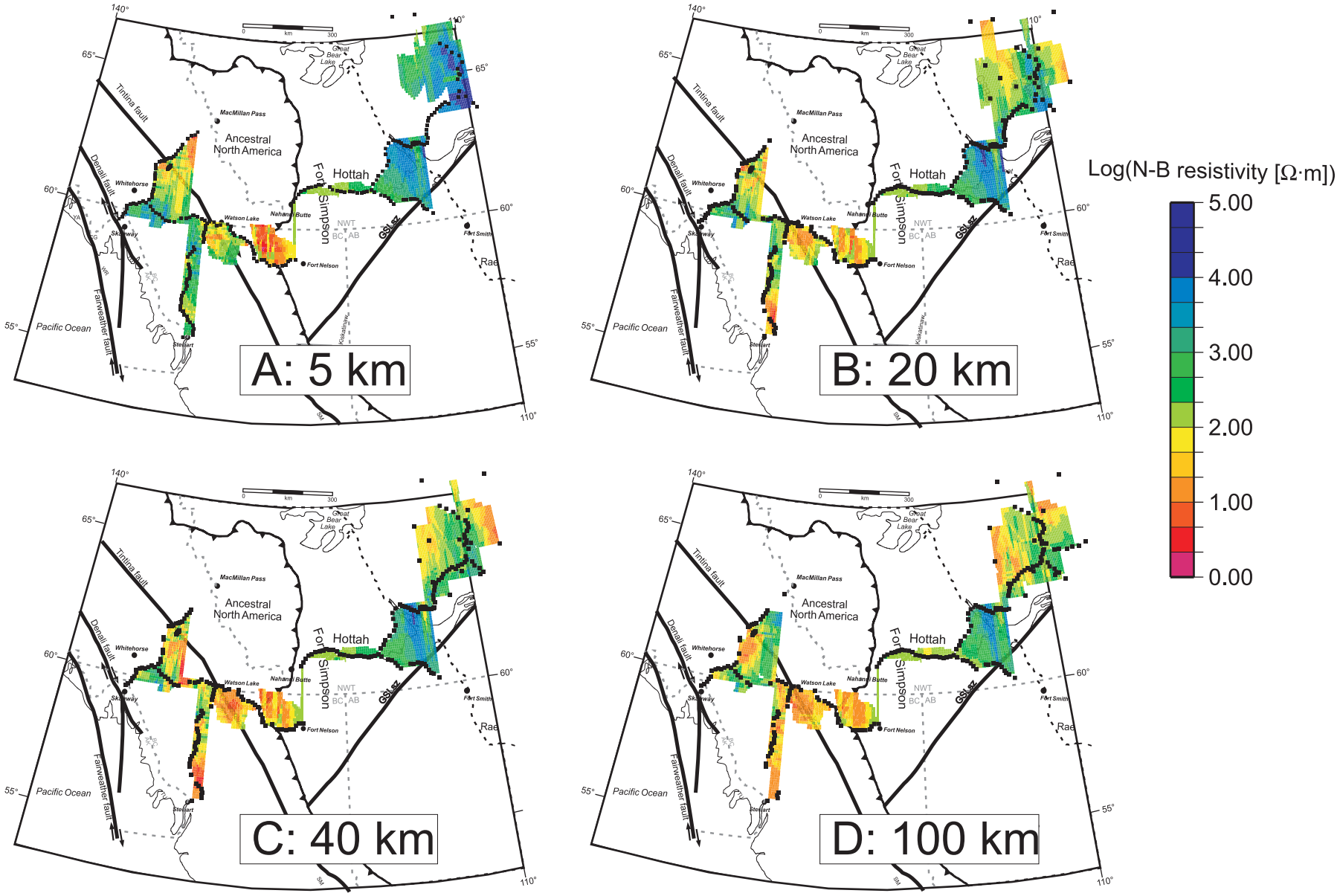

© 2005 NRC Canada

Fig. 5. Maps of percentage resistivity anisotropy at depths of (A) 5 km, (B) 20 km, (C) 40 km, and (D) 100 km.

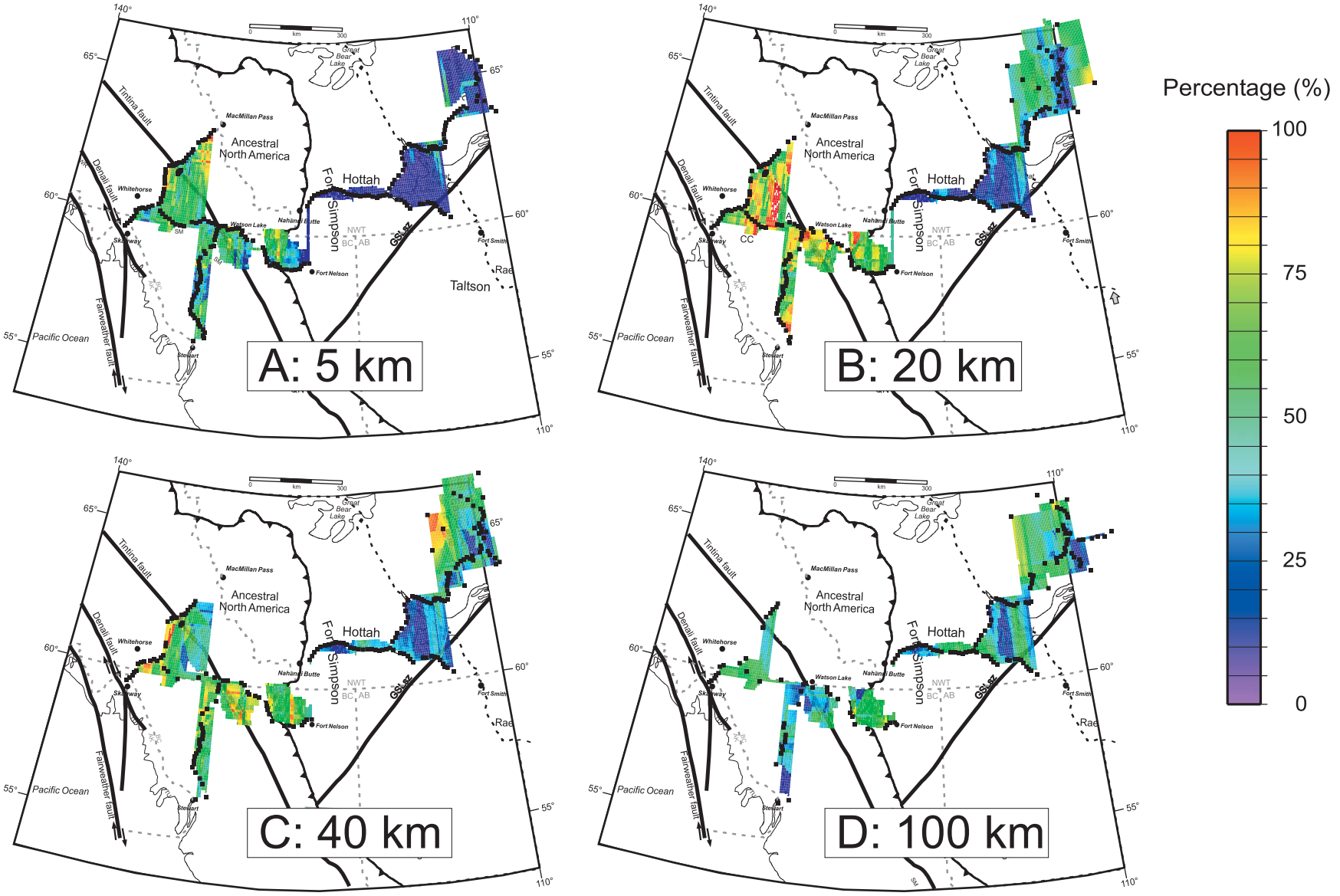

© 2005 NRC Canada

Fig. 6. Resistivity model of the MT data from selected sites along the regional profile shown in Fig. 1 (station locations indicated by ticks on upper border). (*a*) Model in continuous colour scale. (*b*) Model in a colour scale that highlights the low-resistivity (red) and high-resistivity (blue) regions. The eight features labelled A–H are discussed in the text.

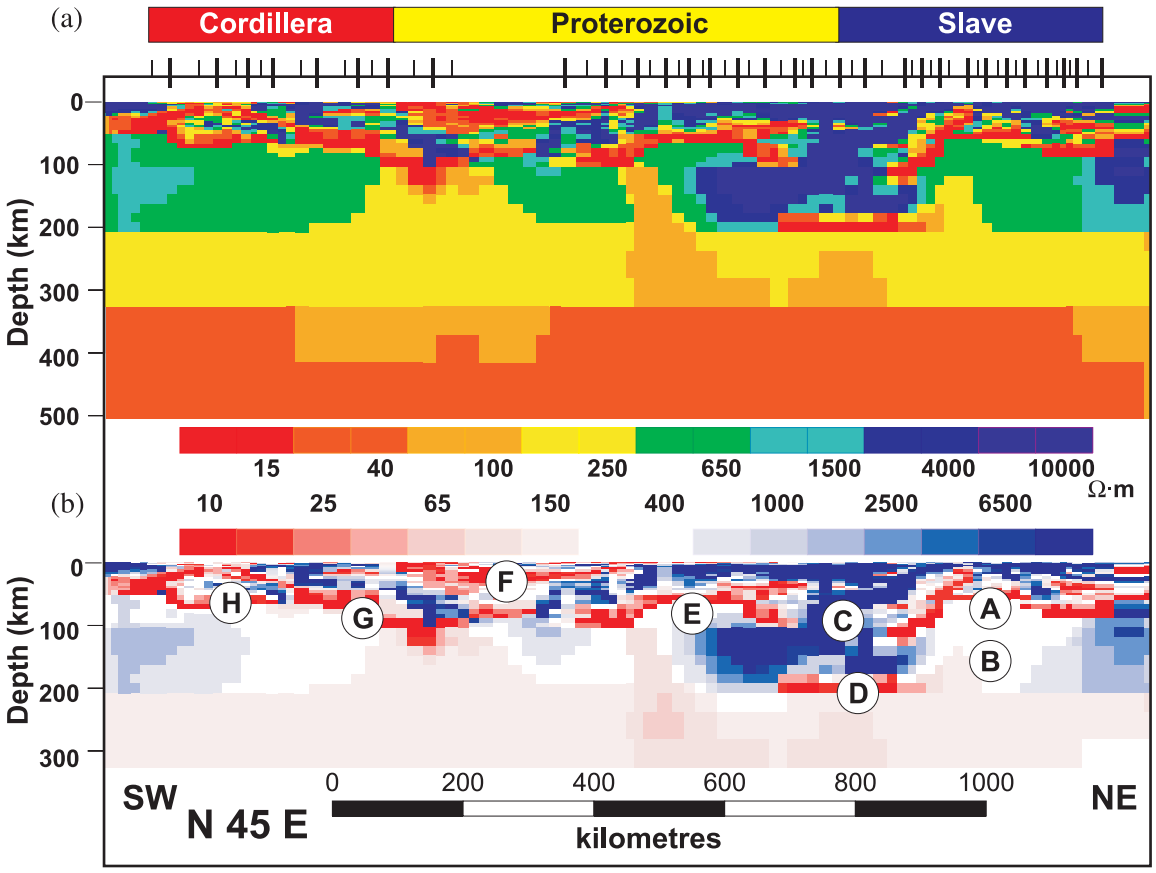

(2) There is a significant difference in deep crustal and upper mantle resistivity structure between corridors 2 and 3. The MT data along corridor 2 gives evidence for a conducting lower crust, similar to the southern Cordillera (Jones et al. 1992; Jones and Gough 1995; Ledo and Jones 2001). However, the lower crust beneath corridor 3 is unusually resistive (Ledo et al. 2004). This difference is discussed further later in the text.

Anisotropy maps

Resistivity anisotropy maps are shown in Fig. 5 for the same depths as previously mentioned, namely 5 km, 20 km, 40 km, and 100 km. The dominant features in the maps are

(1) The Slave craton's crust is isotropic, and the southwestern part of the Slave craton (Anton complex) is isotropic throughout virtually the whole crustal and mantle lithosphere. Although the crust and mantle of the Wopmay orogen along corridors 1 and 1A appears to be isotropic in Fig. 5, the observed response is in large part an artefact of the masking effect of the overlying conductive Phanerozoic sedimentary rocks.
(2) Strong mid-crustal anisotropy is evident at most of the Cordilleran stations.
(3) Anisotropy decreases with increasing depth in the Cordillera.

Regional profile

Construction of 2-D resistivity model

The MT sites along corridors 1S, 1, and 2 were assembled into the single 1600 km-long regional-scale NE–SW profile (profile shown in Fig. 1). Sites were chosen for inclusion and subsequent modelling based on the quality of their data. The MT data were rotated such that the TE-mode responses were for the electric fields directed NW–SE. The TM-mode responses were thus with the electric fields directed NE–SW. The Cordillera exhibits strong resistivity anisotropy (see Fig. 5), and a careful geoelectric strike analysis by Ledo et al. (2004) for the MT data along corridor 3 and by Wennberg et al. (2002) for the data along corridor 2, demonstrated that the appropriate crustal and upper mantle regional strike direction is NW–SE. As shown in Fig. 5, the MT data from the Slave craton show little evidence of strong lateral anisotropy and are thus not significantly affected by choice of strike angle. The appropriate strike angle in the Wopmay orogen is NE–SW (Wu et al. 2005) so the resistivity model for this portion of the regional profile must be interpreted with care. The structures for this part of the profile are shown in more detail in Wu et al. (2005).

Inversion of the MT data used the RLM2DI code of Mackie (Rodi and Mackie 2001), as implemented in Geosystem's WinGLink package. Data from both TE and TM modes in

© 2005 NRC Canada

the frequency range of 100–0.0001 Hz (0.01 – 10 000 s) were modelled. An error floor of 25% was set for the apparent resistivities to constrain static shift effects, whereas the phase error floor was set to 2°. The final model that fits both the TE and TM mode MT responses is shown in Figs. 6. Its normalized root mean square (RMS) misfit is 2.6; thus the model fits the data on average to within 5° of phase, with most of the misfit at the longest periods (>1000 s). Figure 6*a* shows the model with a continuous colour representation, whereas Fig. 6*b* shows the model with the low and high resistivity zones highlighted in red and blue, respectively. The model is shown on a 1:1 scale, and eight dominant features are identified, labelled A–H (see Fig. 6*b*).

Major features of regional resistivity model and interpretation

Feature A

The upper mantle conductor beneath the centre of the Slave craton has been discussed in Jones et al. (2001, 2003) and in Davis et al. (2003), and was named the Central Slave Mantle Conductor (CSMC). This conductor, starting at a depth of ~80–100 km with a thickness extent of some 20–40 km (Jones et al. 2003), is interpreted to be due to graphite or an interconnected carbon grain boundary film. Carbon is conducting above the graphite–diamond stability field, which is interpreted to lie at about 125–140 km for the Slave craton, but highly resistive below it when in diamond form.

Feature B

Penetration by electromagnetic waves into the lithospheric region beneath the CSMC is hindered by the attenuating effects of the CSMC itself, and the winter road LMT responses do not go to sufficiently long enough periods to penetrate through the CSMC to the lithosphere–asthenosphere boundary. Due to its one year installation, the WHOI lake bottom instrument located in Lac de Gras does have high-quality long-period response estimates to 10 000 s, and a 1-D interpretation of them indicates that the maximum permitted resistivity of the lower lithosphere of the central Slave is of the order of 50 Ω.m, with a poorly defined electrical asthenosphere of ca. 5 Ω.m at about 210 km (Jones et al. 2003). This lower lithosphere value, although 3–5 times higher than for the CSMC, is nevertheless more than one and a half orders of magnitude more conducting than dry olivine–pyroxene mineralogy (Xu et al. 2000; Ledo and Jones 2005). In the absence of more plausible candidates, this reduced resistivity we ascribe to hydrogen diffusion (Karato 1990; Hirth et al. 2000). The lithospheric thickness corresponds well with the value of 190 km determined for the central Slave by Pearson et al. (1999).

Feature C

The southwestern Slave Province, including the Anton complex, has highly resistive and isotropic lithosphere as noted earlier. Figs. 4–6 indicate that this response extends some tens of kilometres southwest along corridor 1 into the Wopmay orogen. Although initial examination of Figs. 4 and 5 suggests that the response also extends to the south across corridor 1A, careful examination of the results shows that the resistive and isotropic responses on corridor 1A are associated with the GSLsz and the Buffalo Head terrane, which is located to the east of the shear zone, and that the lithosphere is, in fact, relatively conductive along the western part of that corridor.

Seismic reflection results (Cook et al. 1998, 1999) and teleseismic data (Bostock 1997) have provided some constraints on the geometry of the margin of the Slave Province. Their results suggest that the Great Bear magmatic arc forms a 2–5 km-thick surface layer. The provenance of the Wopmay crust beneath the Great Bear rocks is uncertain and the crust may consist of either Hottah terrane or Coronation Margin rocks or both. The reflectivity pattern in the lower crust is distinct from that in the upper crust and suggests duplication along east-dipping thrust faults with the overall shortening accommodated at the Moho (Cook et al. 1999). The uppermost mantle beneath the Moho is interpreted to be a wedge of Slave mantle extending ~100 km beneath the Wopmay orogen. This wedge is interpreted to be underlain by Wopmay mantle extending some distance beneath the Slave Province (Cook et al. 1998).

The observation of resistive crust immediately southwest of the surface margin of the Slave craton provides additional constraints on the geological interpretation. The resistive crust on corridor 1 is in contrast with the resistivity models for corridor 1A, in which there is a significant crustal conductor at this longitude (Wu et al. 2005), and it is in contrast with the results of Camfield et al. (1989) from the northern Wopmay orogen that revealed a crustal conductor in the Coronation margin. Boerner et al. (1996) interpret the Coronation conductor to be due to graphitic or sulphidic rocks originally deposited in a restricted oceanic environment and subsequently metamorphosed and deformed during the Calderan Orogeny. Our results for corridor 1 appear to exclude the possibility of such rocks being present immediately adjacent to the Slave craton. It therefore appears more probable that the resistive response is because of the wedge of Slave rocks or the presence of Hottah terrane rocks.

The observation of resistive lithospheric mantle in the southwest Slave craton places a powerful constraint on mantle composition. In this region, there can be no interconnected carbon phase beneath this region at depths above the graphite–diamond stability field, in contrast to the interpretation of the CSMC. The extension of the resistive mantle beneath the Wopmay orogen supports the interpretation of the seismic data of a west-penetrating wedge of Slave mantle immediately beneath the Moho.

Feature D

Along the whole profile the electrical asthenosphere is deepest beneath this region of highly resistive lithosphere. The resistivity results suggest that the asthenosphere lies at a depth of some 260 ± 35 km (Jones et al. 2003), which correlates well with the petrologically defined lithospheric thickness of 260 km for the southern Slave by Kopylova (2002). The resistivity models do not resolve any significant change in resistivity at the 75–80 km depth of a mantle reflection tentatively interpreted to form a detachment between Slave lithospheric mantle above and Wopmay lithospheric mantle below (Cook et al. 1998).

© 2005 NRC Canada

Feature E

The regional model resolves relatively high conductivity in the mantle at ~80 km depth beneath the central Wopmay orogen. This enhanced conductivity is also observed in resistivity models derived from MT data projected into a more appropriate orientation for the Wopmay orogen (Wu et al. 2005). There are two alternative interpretations for the enhanced conductivity, either that the conductor represents the electrical asthenosphere and, therefore, the presence of thin mantle lithosphere, or that the conductor represents anomalously conductive mantle lithosphere.

The hypothesis of thin lithosphere is consistent with the elevated heat flow for this region, with a heat flow of 97 mW/m^2 calculated for Fort Providence (Lewis and Hyndman 1998), and an average of 89 ± 17 mW/m^2 for the Hottah, Fort Simpson, and Nahanni terranes (Lewis and Hyndman 1999). Majorowicz (1996) had previously drawn attention to the anomalously high heat province of this region. Using these values a conductive geotherm would suggest a lithospheric thickness of around 100 km, which is in reasonable agreement with the observations. However, it is difficult to explain the relatively abrupt margins of the mantle conductor with this hypothesis; a thermal field would be more transitional.

The alternative hypothesis explaining enhanced conductivity in the Hottah mantle is that it was caused by modification of the mantle associated with subduction during the collision and accretion of the Hottah terrane to the western margin of the Slave craton and subsequent collision of the Fort Simpson terrane. Seismic reflection results show delamination structures extending to 100 km depth into the mantle beneath the Great Bear magmatic arc, providing evidence that lower crustal Hottah rocks were emplaced into the mantle during subduction (Cook et al. 1998, 1999). Seismic refraction results also show an anomalous mantle response in which at depths < 80 km, the velocity is about 7.7 km/s in beneath the Hottah terrane, which is around 0.5 km/s lower than the adjacent areas (Fernández-Viejo et al. 1999; Fernández-Viejo and Clowes 2003). The source of the enhanced conductivity in the Hottah mantle is interpreted to be water and (or) carbon introduced into the mantle through subduction processes. It is significant to note that the top of the conductor, ~60 km, correlates with the minimum depth at which H_2O would become interconnected, according to dihedral wetting angle arguments (Mibe et al. 1998). The observation of calc-alkaline magmatism in the Great Bear magmatic arc indicates that the mantle was hydrated at the time of the Fort Simpson collision, and the observation of the present velocity anomaly suggests the presence of long-term changes in mantle mineralogy. Following Karato (1990) and Hirth et al. (2000), hydrated mantle is expected to exhibit reduced resistivity because of the diffusion of hydrogen.

Feature F

The anomaly marked as F is poorly resolved, given the large gap in station spacing at that location. Nevertheless, there is the indication that the crust is significantly more conducting in this region than elsewhere along the profile. This conductive crust lies in the transitional region between the Wopmay orogen and Cordillera. The basement rocks are covered by Phanerozoic rocks but, as noted earlier in the text, are believed to consist of sequences of Proterozoic passive margin sedimentary rocks (Snyder et al. 2002). In the deeper parts of the crust these rocks will have been metamorphosed to form gneiss and granulites, but if conducting phases exist, such as graphite or sulphides, then they would persist and be detectable.

There may be multiple sources of the enhanced crustal conductivity. Examination of the resistivity model along corridor 1 (Wu et al. 2005; Fig. 6) indicates that the enhanced conductivity occurs in the lower crust. This lower crust, interpreted on the basis of the seismic reflection data to be Fort Simpson terrane crust (Cook et al. 1999) is significantly less resistive (< 200 Ω.m) than the sedimentary sequences in the overlying Fort Simpson basin (> 600 Ω.m), which have been interpreted to be Wernecke Supergroup and Mackenzie Mountain Supergroup rocks (Cook et al. 1999).

The resistivity models for the eastern parts of corridors 2 and 3 both contain conductive rocks. For corridor 3, shallow conductors (< 3 km depth) can be confidently associated with carbonaceous shales and mineralization in the Selwyn basin (Ledo et al. 2004). Deeper conductors at the eastern end of this corridor (resistivity < 10 Ω.m) are located within rocks interpreted to form part of the Proterozoic Windermere and MacKenzie Mountain supergroups (Snyder et al. 2002). The enhanced conductivity may be explained by the presence of conductive rock units within these sequences. However, the Windermere and Mackenzie Mountain supergroups along with the underlying Proterozoic sequences (the Muskwa Assemblage and Wernecke Supergroup) are interpreted to form part of a WTW extending through the middle and lower crust beneath corridors 2 and 3. As shown in Figs. 6 and 7, and in more detailed modelling studies (Ledo et al. 2004, Wennberg et al. 2002), this purported wedge, if it exists, does not form an extensive conductor (see further discussion later in text).

It is of note that several isolated conductors in the Omineca Belt and the enhanced conductivity at the northeast of corridors 2 and 3 lie near the interpreted upper margin of the Proterozoic wedge. It is possible that both sets of conductors have a similar origin, and are associated with the deformation that occurred during the Cordilleran thrusting of younger rocks over the Proterozoic crustal wedge.

Feature G

There is a northeast-dipping conducting layer identified in the Cordillera that can be traced from the mid-crust deep into the lithosphere. The simplest geometrical interpretation of this feature is to associate it with lithospheric subduction during terrane accretion. This feature is discussed in more detail below.

Feature H

Beneath the southwestern part of the profile the electrical lithosphere is thin, again consistent with the heat flow data (Lewis and Hyndman 1999).

Comparison between corridors 2 and 3

The resistivity maps in Fig. 4 suggest there are both significant similarities and differences in the electrical structure along corridor 3 and a composite corridor 2. The upper lithospheric portion from the regional model of Fig. 6 can be

© 2005 NRC Canada

Fig. 7. (*a*) Two-dimensional resistivity model obtained by inversion of both the TE- and TM-mode resistivities and phases along corridor 3. CB, Coast Belt; IB, Intermontane Belt; TsF, Teslin Fault; OB, Omenica Belt; TTF, Tintina Fault; ANA, Ancestral North America. The westward-tapering wedge (WTW) of Cook et al. (2004) is also shown, as is the location of the Moho. Inverted triangles show the position of the MT sites (from Ledo et al. 2002). (*b*) Part of the composite corridor 1 + 2 model of Fig. 6 that compares spatially with corridor 3. The location of the WTW and Moho have been projected from corridor 3 onto composite corridor 2. Features labelled 1–3 are discussed in the text.

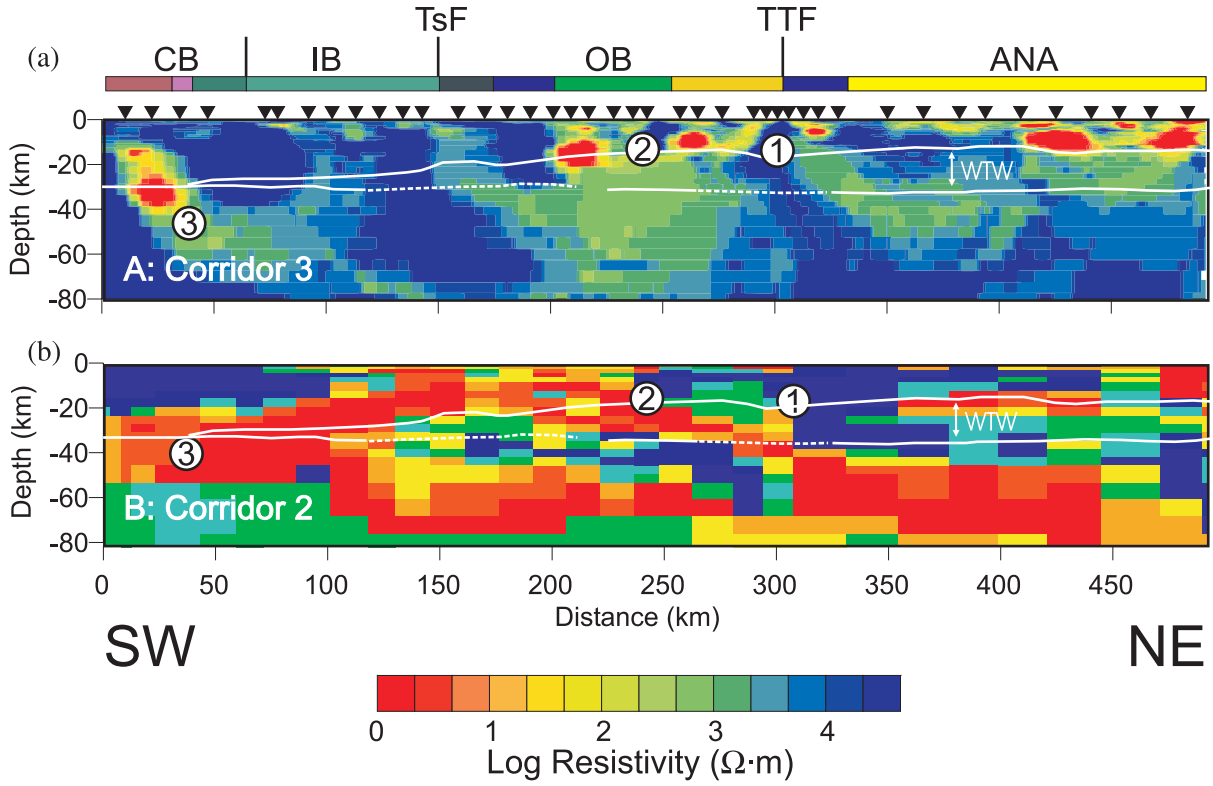

compared with the more detailed model of the corridor 3 profile recently presented by Ledo et al. (2004). The composite corridor 2 model (Fig. 7*b*) has far greater cell dimensions at this scale, compared with the corridor 3 model (Fig. 7*a*). However, the significant difference between the two will not change when the corridor 2 data are modelled with the same level of block discretization. Also shown on Fig. 7 are the traces of the WTW and the Moho. The positions of these are correct for corridor 3 (taken from Ledo et al. 2004), but have been projected from corridor 3 onto composite corridor 2.

The most significant difference in electrical structure between the two corridors is that beneath corridor 2 the crust and uppermost mantle are far less resistive (more conducting), than beneath corridor 3. Clearly, the Cordillera is not uniform along strike in its electrical structure, which implies that it is unlikely to be uniform along strike in its fluid content, thermal structure, rheology, and orogenic processes.

This result can be compared with the heat flow data of Lewis et al. (2003) that show far higher heat flow values north of 59° compared with south of it; namely 105 ± 22 mW/m^2 compared with 73 ± 11 mW/m^2, respectively. Lewis et al. (2003) attribute this north–south difference as primarily due to higher upper crustal heat generation north of 59°. The conductive geotherm calculated for north of 59° is higher than that for south of 59°, but because of the large range of heat flow and heat generation values this difference cannot be demonstrated to be statistically significant. The evidence from our result though is that there is reason to believe that there is a significant difference north of 59°.

There are a number of significant similarities between the resistivity models for the two corridors:

(1) The resistivity structure of the Tintina Fault (TTF) is remarkably similar on corridors 2 and 3, shown in more detail in Fig. 7, and on a short high-density profile 35 km south of corridor 3 (model not shown). The resistivity models for all three profiles exhibit several high-conductivity structures (~1–10 Ω.m) with vertical contacts below the surface trace of the TTF up to 5 km depth that can be spatially associated with the fault system (labelled as feature 1 in Fig. 7). At deeper levels (below 5 km) to the southwest of the fault, a significant conductivity structure (~1 Ω.m) is present and to the northeast another conductive structure is identified. Finally, a common feature of the three models is the occurrence of a highly resistive zone at deep crustal levels below the surface trace of the TTF. Ledo et al. (2002) discuss these structures in more detail. The results suggest 2-D electromagnetic behaviour of the TTF over a strike length of at least 400 km, i.e., from corridor 2 to corridor 3. The fault is imaged as a subvertical crustal-scale high-resistivity feature throughout its whole crustal extent along the three MT profiles. Comparison of the seismic reflection data (Cook et al. 2001, 2004) and the

© 2005 NRC Canada

resistivity model for corridor 3 (Fig. 7) shows a good correlation between the high-resistivity zone and the absence of reflectors. The coincidence of fault zones transparent to both seismic and electrical methods implies that the fault could be considered potentially healed (Eberhart-Phillips et al. 1995).

(2) Along both corridors 2 and 3, upper crustal conductors are observed at 10–20 km depth in the Omineca Belt (Cassiar terrane), labelled as features 2 in Fig. 7. These conductors can be seen in the corridor 3 profile in Fig. 7, but for corridor 2 are shown more clearly in the detailed resistivity models of Wennberg et al. (2002) than in the lower resolution model for corridor 2 in Fig. 7. As noted earlier in the text, these conductors appear to lie close to the upper surface of the putative WTW of Proterozoic rocks and may be associated with the deformation that occurred during the thrusting of Cordilleran terranes over the wedge.

(3) A similar northeast-dipping conductor is observed near the southwestern ends of corridors 2 and 3 (Wolynec 2000; Wennberg 2003; Ledo et al. 2004), labelled as feature 3 in Fig. 7. Along both corridors this conductor dips from crustal to mantle depths. The depth to the top of the conductor on line 3 (> 10 km) is shallower than the depth of the conductor on line 2a (> 20 km), but this difference may be explained by the position of the lines. The dip of the structure imaged on line 2a is shallower than the dip on line 3, but this difference may be explained by the oblique orientation of line 3 relative to the coast. The results therefore suggest that the same or a very similar body is being imaged on corridors 2 and 3. Ledo et al. (2004) provide an interpretation of this dipping structure and compare it with a lower crustal conductor observed to the north in Alaska (Stanley et al. 1990). The northeast-dipping conductor on the SNORCLE transect lies above, and parallel to, a suite of reflectors located at mantle depths that were interpreted by Cook et al. (2001, 2004) to be associated with convergent subduction of the Kula plate in the Paleocene (Engebretson et al. 1984). The coincidence of the geometry of the conductor and the inferred position of the subducting slab provides a strong indication that the decreased resistivity is related to the Paleocene Kula plate subduction. The original explanation of the Alaskan Range conductor was that it was due to metasedimentary rocks emplaced into the deeper crust by the underthrusting of carbonaceous flysch during mid-Cretaceous convergence (Stanley et al. 1990). Ledo et al. (2004) suggest that the crustal part of the conductor observed on corridors 2 and 3 may also be metasedimentary rocks imbricated during Kula plate subduction. The resistivity of the mantle part of the dipping conductor (300–1000 Ω.m) is less than for the crustal part (3–30 Ω.m), and it is possible that the mechanism causing the decreased resistivity is different in the two regions. Ledo et al. (2004) propose that the enhanced mantle conductivity is caused by the introduction of H_2O-bearing fluids into the mantle wedge overlying the subducting slab. The conductivity may be enhanced by either the presence of hydrous minerals or more likely the addition of small amounts of water to nominally anhydrous minerals (Karato 1990), as in the interpretation of the enhanced conductivity in the Hottah mantle and in the mantle lithosphere beneath the CSMC.

Comparison of electrical models with seismic reflection interpretation

One key interpretation of the SNORCLE northern Cordillera seismic reflection data is the presence of a westward-tapering lower crustal wedge (WTW) of prominent reflectivity (Cook et al. 2001, 2004, 2005; Snyder et al. 2002), described as a lower crustal layered sequence (LCLS), that has been interpreted as Proterozoic sediments (Snyder et al. 2002), possibly with involvement of pre-1.8 Ga basement (Cook et al. 2004). Such a tapering wedge interpretation is similar to the one proposed by Cook et al. (1992) for the southern Canadian Cordillera, although in the southern Cordillera data there was a prominent and continuous subhorizontal reflector marking the top of the wedge. The position of the Moho, inferred as the crust–mantle transition, is defined on the seismic reflection sections by a sharp decrease in reflectivity at about 11.5 s two-way traveltime, although along corridor 3, it is somewhat diffuse in the vicinity of the TTF and also shows variation on the seismic reflection pattern below the Intermontane Belt. Another important result is the absence of strong laterally continuous crustal reflectors below the surface trace of the TTF.

The geometry of the WTW is shown in Fig. 7 on both resistivity models, together with the Moho. This geometry is taken for the corridor 3 profile (Ledo et al. 2004) and is projected onto the composite corridor 2 model. Although Cook et al., and Snyder et al. chose to regard the WTW as indicative of a continuous geological feature, we note that the WTW is not continuous, and is, in parts, defined by the onset of reflectivity, rather than by a subhorizontal reflector or package of reflectors. In particular, west of the TTF, within the WTW, the LCLS reflectors are east-dipping (see foldouts 2 and 3, and in particular fig. 9, in Cook et al. 2004).

Discussion

The model shown in Fig. 6 depicts the regional electrical structure from the northeastern part of the Slave craton to the North American coast across Archean, Proterozoic, and Phanerozoic structures that record orogenesis throughout much of Earth's history. The large scale features A–H in Fig. 6, discussed earlier in the text, are considered to be robust in that further processing, analyses, and modelling of the data are unlikely to modify them significantly. The conductive features must exist approximately where they are, although details, such as the angle of the dip of feature G, may change. Note that although this is a regional 2-D model, the region is clearly 3-D, as evident in the difference between corridors 2 and 3. However, each of the features is imaged as virtually separate entities, implying no mutual interaction between them.

Significantly enhanced conductivity is observed at crustal and mantle depths over much of the regional profile. The only exception is in the southwest part of the Slave craton where the resistivity results show that the crust of the Anton complex and the underlying lithosphere is extremely resistive, allowing the conclusions to be drawn that the crust and

© 2005 NRC Canada

mantle have not been hydrated and that, above the depth of the diamond stability field, they are devoid of graphite.

It is of note that many of the conductive anomalies observed on the regional profile record episodes of crustal accretion: these conductors are interpreted to be due to the introduction of water, sulphides and (or) graphite into the crust and mantle during subduction. The CSMC has been interpreted to be due to the emplacement of oceanic or arc-related lithosphere emplaced during early tectonism (Jones et al. 2001, 2003; Davis et al. 2003). Deformation and plutonism at 2630–2620 Ma restricted to the southern part of the newly amalgamated Slave craton record the subduction of a craton of unknown provenance to the south beneath the southern Slave (Bleeker et al. 1999*a*), and this event would provide the appropriate mantle geometry of the geophysical anomaly and also the related geochemical anomaly. The enhanced conductivity of the mantle beneath the Hottah terrane has been interpreted on the basis of mantle reflectivity to be due to hydration associated with subduction of Fort Simpson crust (Wu et al. 2005). Finally, the enhanced conductivity in the crust and mantle observed in the dipping feature at the southwest end of the SNORCLE transect have been interpreted to be associated with the subduction of the Kula plate.

The interpretations just made for Wopmay and Cordillera conductors were permitted in part by a correlation of electrical resistivity and mantle reflectivity. In other areas of the SNORCLE transect there is a notable lack of correlation between reflectivity and resistivity images. For example, one of the major features of crustal reflectivity, the WTW of crustal reflectivity (Cook et al. 2001, 2004; Snyder et al. 2002), interpreted to correspond to Proterozoic passive margin sediments, has no clear resistivity signature. If the tectonic model of Cook et al. (2004) is correct, then there are two likely end members to explain this: (1) The electrical resistivity variations within the wedge, associated with North America lower crust, are inherent to the origin of the Proterozoic sediments or (2) these variations arose during the subsequent Cordilleran accretionary episodes because of redistribution of conductive material, caused by changes in stress fields and migration of fluids and partial melting from the lithosphere of subducted terranes (Ledo et al. 2004). However, our conclusion is that our data suggest an alternative accretionary model.

Comparing the seismic reflection interpretation of the WTW with our own models (Fig. 7), we do not see consensus. Given the east-dipping geometry of our major feature G along composite corridor 2 (Figs. 6, 7), and of the dominant terrane pattern along corridor 3 (Fig. 7), we conclude that the MT data do not support the model for the development of the northern Cordillera proposed by Cook et al. (2004) of accretion of thin flakes on a WTW of Proterozoic strata with their basement (foldout 4 in Cook et al. 2004). Our models suggest, in contrast, involvement of terranes that had significant crustal extent.

We note that the east-dipping LCLS reflectivity within the WTW is consistent with the east dip of feature G in our regional model (Fig. 6). As is common with almost all reflection sections, reflectivity is abruptly curtailed at the Moho with the impression of the LCLS reflectors becoming listric into the sharp Moho. However, feature G in our model suggests that structures indeed traverse the Moho and that the Moho is not a major décollement to tectonic structures but only to reflection data.

Research into the source of differences between the resistivity models along corridors 2 and 3 is ongoing. The results are enigmatic in that they show remarkable similarities of some smaller scale features, such as the resistivity structure of the TTF and localized conductors in the Omineca Belt, while showing differences in the large-scale resistivity of the crust and mantle. At crustal depths, one of the important differences may be the presence of a much more extensive component of Stikinia, one of the largest terranes of the Cordillera, on corridor 2. The source of the different resistivity at mantle depths is likely tied to variations in other geophysical responses, including heat flow (Lewis and Hyndman 1999, 2001) and large-scale seismic velocity (Frederiksen et al. 1998). Detailed modelling and inversion employing identical inversion algorithms and parameters will be used to define precisely the differences between the resistivity models for the two profiles, and comparisons with both geological and geophysical data will be used in the interpretation.

Conclusions

The SNORCLE magnetotelluric investigations have been undertaken in three different modes to study different aspects related to the actual state and evolution of the northern Canadian Cordillera and Slave craton.

The first mode involves characterization of the lithospheric-scale resistivity properties along the transect. This objective has been achieved at a whole transect scale through the electrical resistivity maps presented in this paper. The main features obtained from this semi-quantitative approach have been corroborated by the regional 2-D inversion models obtained. One of the components of this work was the delineation of the depth to the electrical asthenosphere. The results have shown, for example, that this depth is around 190 km in the central Slave craton, 260 km in the southwest Slave Province, and significantly < 100 km at the southwestern end of corridors 2 and 3. Note that these are not the depths to the first mantle conductor, but to what we associate with the base of the lithosphere. In the case of the centre of the Slave craton, the Central Slave Mantle Conductor (CSMC) at a depth of some 80 km is not the asthenosphere, which lies at 190–200 km depth deduced from the very long-period lake bottom data (Jones et al. 2003). However, in a number of areas of the SNORCLE transect enhanced conductivity in the crust and upper mantle has restricted the ability to resolve the depth to the asthenosphere.

Previous studies (Jones et al. 2001, 2003; Ledo et al. 2004, Wu et al. 2005; Jones and Garcia 2005, Wennberg 2003) have characterized the resistivity properties along each of the transect corridors at a smaller scale. These results allow the division of the Slave craton into one area characterized by a major regional mantle conductivity anomaly and a second area in the southwest characterized by extremely resistive crust and lithosphere. Several terrane boundaries within the Proterozoic Wopmay orogen are characterized by enhanced conductivity (Wu et al. 2005), and the mantle beneath the centre of the orogen is characterized by enhanced conductivity. The resistivity character of belts and terranes of the northern

© 2005 NRC Canada

Cordillera has also been defined; for example, the presence of localized conductors in the Cassiar terrane of the Omineca Belt (Ledo et al. 2004).

The second mode of analysis of SNORCLE MT data has involved the extraction of geological information from the resistivity images. As a qualitative example of this work, the CSMC can be used to define a region of the Slave mantle affected by late Archean tectonism. As a quantitative example for corridor 3, the high resistivity mantle observed below the Intermontane Belt has been related to thermal and mineralogical properties by Ledo and Jones (2005) by using appropriate mixing relationships for olivine, orthopyroxene, and clinopyroxene to construct mantle rock resistivities. The work demonstrated that the upper mantle temperature of the Intermontane Belt along corridor 3 is bounded between 850 and 1050 °C, which is some 200 °C lower than that proposed by Frederiksen et al. (1998).

Perhaps our most significant result though is the disparity we see between our east-dipping feature G on composite corridor 2 and the block structure of resistivity on corridor 2 with the westward-tapering wedge of Cook et al. (2001, 2004, this issue), with its consequent inference of the terranes of the Cordillera being thin flakes. In contract, our models suggest significant crustal extent to the terranes that docked with ancestral North America.

The final mode of analysis of SNORCLE MT data has involved the smallest scale objective of this study, resolution of the structure of major faults. The Tintina strike-slip fault zone has been characterized electrically, the main result is the presence of a high resistivity anomaly below the surface trace of the fault that broadens with depth (Ledo et al. 2002). The GSLsz has also been imaged and shown to form a crustal-scale feature with the fault itself characterized by an anomalously resistive zone (Wu et al. 2002).

The ~300 MT sites on the SNORCLE transect have provided a source of information for investigating the Archean to Tertiary aged lithosphere and tectonic structures along the transect. Analysis of the data set is continuing, in particular investigations into the source of north–south differences in resistivity in the northern Cordillera and better definition of resistive features.

Acknowledgments

Financial support for the SNORCLE EM activities came from Lithoprobe, Geological Survey of Canada, Canadian Federal Department of Indian and Northern Development (DIAND), the US. National Science Foundation, Monopros (now De Beers Exploration Canada), Kennecott, and BHP. Student and postdoctoral support was provided by Lithoprobe, the GSC, and the Natural Sciences and Engineering Council of Canada. We are particularly grateful for the contributions of Alan Chave and Rob Evans from Woods Hole Oceanographic Institute, which enabled the collection of data from the northern Slave craton.

Phoenix Geophysics Ltd. and Geosystem Canada Ltd. are both thanked for their support in terms of reduced academic survey rates and their attention to detail resulting in high quality responses. For the Slave studies accommodation was provided along the winter roads by Diavik, BHP, Monopros, and Winspear, and in Yellowknife by Royal Oak Mines and Miramar Mining. The staff of the Yellowknife Seismological Observatory is thanked for its support, for providing essential preparation facilities, and provision of magnetic observatory recordings. Finally, we wish to thank our colleagues, especially Wouter Bleeker, Bill Davis, and Herman Grutter, for enlightening discussions, and the reviewers, Toivo Korja and Heinrich Brasse, and Associate Editor Ron Clowes for their very useful comments on our submitted version of this paper.

References

Aitken, J.D. 1993. Cambrian and lower Ordovician-Sauk sequence. In Sedimentary cover craton in Canada. *Edited by* D.F. Stott and J.D. Aitken. Geological Survey of Canada, Geology of Canada, no. 5, Chap. 4B, pp. 96–124.

Andersen, F., Boerner, D.B., Harding, K., Jones, A.G., Kurtz, R.D., Parmelee, J., and Trigg, D. 1988. LIMS: Long period intelligent magnetotelluric system. Contributed paper at 9th Workshop on EM Induction Sochi, USSR, 24–31 October 1988.

Aspler, L.B., Pilkington, M., and Miles, W.F. 2003. Interpretations of Precambrian basement based on recent aeromagnetic data, Mackenzie Valley, Northwest Territories. Geological Survey of Canada Current Research, 2003-C2, 11 p.

Bahr, K., and Simpson, F. 2002. Electrical anisotropy below slow- and fast-moving plates: paleoflow in the upper mantle? Science (Washington, D.C.), **295**: 1270–1272.

Berdichevsky, M.N., and Dmitriev, V.I. 1976. Basic principles of interpretation of magnetotelluric sounding curves. *In* Geoelectric and geothermal studies. *Edited by* A. Adam. KAPG Geophysical Monograph, Akadémiai Kiadó, Budapest, Hungary, pp. 165–221.

Bleeker, W., Ketchum, J.W.F., Jackson, V.A., and Villeneuve, M.E. 1999a. The Central Slave Basement Complex; Part I, Its structural topology and autochthonous cover. Canadian Journal of Earth Sciences, **36**: 1083–1109.

Bleeker, W., Ketchum, J.W.F., and Davis, W.J. 1999b. The Central Slave Basement Complex, Part II: age and tectonic significance of high-strain zones along the basement-cover contact. Canadian Journal of Earth Sciences, **36**: 1111–1130.

Boerner, D., Kurtz, R., and Craven, J.A. 1996. Electrical conductivity and Paleo-Proterozoic foredeeps. Journal of Geophysical Research, **101**: 13 775 – 13 791.

Bostick, F.X. 1977. A simple almost exact method of MT analysis. *In* Workshop on electrical methods in geothermal exploration. US.Geological Survey, Contract No. 14080001-8-359. Reprinted in Vozoff (1986).

Bostock, M.J. 1997. Anisotropic upper mantle stratigraphy and architecture of the Slave craton, Nature (London), **390**: 392–395.

Camfield, P.A., Gupta, J.C., Jones, A.G., Kurtz, R.D., Krentz, D.H., Ostrowski, J.A., and Craven, J.A. 1989. Electromagnetic sounding and crustal electrical conductivity in the region of the Wopmay Orogen, Northwest Territories, Canada. Canadian Journal of Earth Science, **26**: 2295–2395.

Clowes, R.M. (*Editor*). 1993. Lithoprobe phase IV proposal — studies of the evolution of a continent. Lithoprobe Secretariat, The University of British Columbia, Vancouver, B.C., 290 p.

Clowes, R.M. (*Editor*). 1997. Lithoprobe phase V proposal — evolution of a continent revealed. Lithoprobe Secretariat, The University of British Columbia, Vancouver, B.C., 292 p.

Cook, F.A., Varsek, J.L., Clowes, R.M., Kanasewich, E.R., Spencer, C.P., Parrish, R.R., Brown, R.L., Carr, S.D., Johnson, B.J., and Price, R.A. 1992. Lithoprobe crustal reflection cross section of

© 2005 NRC Canada

the southern Canadian cordillera I: foreland thrust and fold belt to Fraser River Fault. Tectonics, **11**: 12–35.

Cook, F.A., van der Velden, A.J., Hall, K.W., and Roberts, B.J. 1998. Tectonic delamination and subcrustal imbrication of the Precambrian lithosphere in northwestern Canada mapped by Lithoprobe. Geology, **26**: 839–842.

Cook, F.A., Van der Velden, A.J., Hall, K.W., and Roberts, B.J. 1999. Frozen subduction in Canada's Northwest Territories: Lithoprobe deep lithospheric reflection profiling of the western Canadian Shield. Tectonics, **18**: 1–24.

Cook, F.A., Clowes, R.M., Snyder, D.B., van der Verden, A.J., Hall, K.W., Erdemer, P., and Evenchick, C. 2001. LITHOPROBE seismic reflection profiling of the northern Canadian Cordillera: first results of the SNORCLE profiles 2 and 3. *In* SNORCLE Transect and Cordilleran Tectonics Workshop Meeting, Sidney, B.C., 25–27 Feb. 2001. *Compiled by* F. Cook and P. Erdmer. Lithoprobe Secretariat, The University of British Columbia, Vancouver, B.C., Lithoprobe Report No. 79, pp. 36–49.

Cook, F.A., Clowes, R.M., Snyder, D.B., van der Velden, A.J., Hall, K.W., Erdmer, P., and Evenchick, C.A. 2004. Precambrian crust beneath the Mesozoic northern Canadian Cordillera discovered by Lithoprobe seismic reflection profiling. Tectonics, **23**: TC2010, doi:10.1029/2002TC001412.

Davis, W.J., and Bleeker, W. 1999. Timing of plutonism, deformation, and metamorphism in the Yellowknife Domain, Slave Province, Canada. Canadian Journal of Earth Sciences, **36**: 1169–1187.

Davis, W.J., Jones, A.G., Bleeker W., and Grütter, H. 2003. Lithospheric development in the Slave Craton: a linked crustal and mantle perspective. Lithos, **71**: 575–589.

Eaton, D.W., and Hope, J. 2003. Structure of the crust and upper mantle of the Great Slave Lake shear zone, northwestern Canada, from teleseismic analysis and gravity modeling, Canadian Journal of Earth Science, **40**: 1203–1218.

Eaton, D.W., Jones, A.G., and Ferguson, I.J. 2004. Lithospheric anisotropy structure inferred from collocated teleseismic and magnetotelluric observations: Great Slave Lake shear zone, northern Canada. Geophysical Research Letters, **31**: L19614, doi:10.1029/2004GL020939.

Eberhart-Phillips, D., Stanley, W.D., Rodriguez, B.D., and Lutter, W.J. 1995. Surface seismic and electrical methods to detect fluids related to faulting, Journal of Geophysical Research, **100**: 12 919 – 12 936.

Engebretson, D.C., Cox, A., and Gordon, R.G.1984. Relative motions between oceanic plates of the pacific basin, Journal of Geophysical Research, **89**: 10 291 – 10 310.

Fernández-Viejo, G., and Clowes, R.M. 2003. Lithospheric structure beneath the Archaean Slave Province and Proterozoic Wopmay orogen, northwestern Canada from a LITHOPROBE refraction/wide-angle reflection survey. Geophysical Journal International, **153**: 1–19.

Fernández-Viejo, G., Clowes, R.M., and Amor, J.R. 1999. Imaging the lithospheric mantle in northwestern Canada with seismic wide-angle reflections. Geophysical Research Letters, **26**: 2809–2812.

Fipke, C.E., Dummett, H.T., Moore, R.O., Carlson, J.A., Ashley, R.M., Gurney, J.J., Kirkley, M.B. 1995. History of the discovery of diamondiferous kimberlites in the Northwest Territories, Canada. *In* Proceedings of 6th International Kimberlite Conference; Novosibirsk, Russian Federation, August 1995.

Frederiksen, A.W., Bostock, M.G., VanDecar, J.C., and Cassidy, J.F. 1998. Seismic structure of the. upper mantle beneath the northern Canadian Cordillera from teleseismic travel-time inversion. Tectonophysics, **294**: 43–55.

Gabrielse, H., and Yorath, C.J. 1991. Introduction. *In* Geology of the Cordilleran Orogen in Canada. *Edited by* H. Gabrielse and C.J. Yorath. Geological Society of America, Geology of North America, Vol. G-2 (also Geological Survey of Canada, Geology of Canada, no. 4), pp. 3–11.

Gordey, S.P., and Anderson, R.G. 1993. Evolution of the northern Cordilleran Miogeocline, Nahanni map area (105I), Yukon and Northwest Territories, Geological Survey of Canada, Ottawa, Ont., Memoir 428.

Griffin, W.L., Doyle, B.J., Ryan, C.G., Pearson, N.J., O'Reilly, S., Davies, R., Kivi, K., van Achterbergh, E., and Natapov, L.M. 1999. Layered mantle lithosphere in the Lac de Gras area, Slave craton: composition, structure and origin. Journal of Petrology, **40**: 705–727.

Hanmer, S., Bowring, S., Breemen, O., and Parrish, R. 1992. Great Slave Lake shear zone, NW Canada: mylonitic record of early Proterozoic continental convergence, collision and indentation. Journal of Structural Geology, **14**: 757–773.

Heinson, G. 1999. Electromagnetic studies of the lithosphere and asthenosphere. Surveys in Geophysics, **20**: 229–255.

Hildebrand, R.S., Hoffman, P.F., and Bowring, S.A. 1987. Tectonomagmatic evolution of the 1.9-Ga Great Bear magmatic zone, Wopmay orogen, northwestern Canada. Journal of Volcanology and Geothermal Research, **32**: 99–118.

Hirth, G., Evans, R.L., and Chave, A.D. 2000. Comparison of continental and oceanic mantle electrical conductivity: Is the Archean lithosphere dry? Geochemistry, Geophysics, Geosystems, **1:** 2000GC000048.

Hoffman, P.F. 1987. Continental transform tectonics: Great Slave Lake Shear zone (1.9 Ga), northwest Canada, Geology, **15**: 785–788.

Hoffman, P.F. 1989. Precambrian geology and tectonic history of North American. *In* Geology of North America — an overview. Geological Society of America, Geology of North America, Vol. A, Chap. 16, pp. 447–512.

Hoffman, P.F., and Bowring, S.A. 1984. Short-lived 1.9 Ga continental margin and its destruction, Wopmay orogen, northwest Canada. Geology, **12**: 68–72.

Jones, A.G. 1983. On the equivalence of the "Niblett" and "Bostick" transformations in the magnetotelluric method. Journal of Geophysics, **53**: 72–73. Reprinted in Vozoff (1986).

Jones, A.G. 1988. Static shift of magnetotelluric data and its removal in a sedimentary basin environment. Geophysics, **53**: 967–978.

Jones, A.G. 1993. The COPROD2 dataset: Tectonic setting, recorded MT data and comparison of models. Journal of Geomagnetism and Geoelectricity, **45**: 933–955.

Jones, A.G. 1998. Waves of the future: superior inferences from collocated seismic and electromagnetic experiments. Tectonophysics, **286**: 273–298.

Jones, A.G. 1999. Imaging the continental upper mantle using electromagnetic methods. Lithos, **48**, 57–80.

Jones, A.G. 2002. Looking into the Earth with polarizing spectacles. Contributed paper presented at the 16th EM Induction Workshop, College of Santa Fe, Santa Fe, N.M., 16–22 June 2002.

Jones, A.G., and Craven, J.A. 1990. The North American Central Plains conductivity anomaly and its correlation with gravity, magnetics, seismic, and heat flow data in the Province of Saskatchewan. Physics of the Earth and Planetary Interiors, **60**: 169–194.

Jones, A.G., and Craven, J.A. 2004. Area selection for diamond exploration using deep-probing electromagnetic surveying. Lithos, **77**: 765–782.

Jones, A.G., and Ferguson, I.J. 1997. Results from 1996 MT studies along SNORCLE profiles 1 and 1A. *In* SNORCLE Transect and

© 2005 NRC Canada

Cordilleran Tectonics Workshop, University of Calgary, Calgary, Alta., 7–9 March 1997. Lithoprobe Secretariat, The University of British Columbia, Vancouver, B.C., Lithoprobe Report 56, pp. 42–47.

Jones, A.G., and Ferguson, I.J. 2001. The electric Moho. Nature (London), **409**: 331–333.

Jones, A.G., and Garcia, X. 2005. Electrical resistivity structure of the Yellowknife River Fault Zone and surrounding region. *In* Gold in the Yellowknife Greenstone Belt, Northwest Territories: Results of the EXTECH-III Multidisciplinary Research Project. Geological Association of Canada, Mineral Deposits Division, Special Publication, in press.

Jones, A.G., and Gough, D.I. 1995. Electromagnetic studies in southern and central Canadian Cordillera. Canadian Journal of Earth Sciences, **32**: 1541–1563.

Jones, A.G., and Spratt, J. 2002. A simple method for deriving the uniform field MT responses in auroral zones. Earth, Planets and Space, **54**: 443–450.

Jones, A.G., Gough, D.I., Kurtz, R.D., DeLaurier, J.M., Boerner, D.E., Craven, J.A., Ellis, R.G., and McNeice, G.W. 1992. Electromagnetic images of regional structure in the southern Canadian Cordillera. Geophysical Research Letters, **12**: 2373–2376.

Jones, A.G., Craven, J.A., McNeice, G.A., Ferguson, I.J., Boyce, T., Farquharson, C., and Ellis, R.G. 1993. The North American Central Plains conductivity anomaly within the Trans-Hudson orogen in northern Saskatchewan. Geology, **21**: 1027–1030.

Jones, A.G., Ferguson, I.J., Chave, A.D., Evans, I.J., and McNeice, G.W. 2001. The electric lithosphere of the Slave craton. Geology, **29**: 423–426.

Jones, A.G., Lezaeta, P., Ferguson, I.J., Chave, A.D., Evans, R.L., Garcia, X., and Spratt, J. 2003. The electrical structure of the Slave craton. Lithos**, 71**: 505–527.

Karato, S. 1990. The role of hydrogen in the electrical conductivity of the upper mantle. Nature (London), **347**: 272–273.

Kopylova, M.G. 2002. The deep structures of the Slave Craton. Presented at "Diamond Short Course," Vancouver, B.C., 21 February 2002.

Korja, T., and the BEAR Working Group. 2003. Upper mantle conductivity in Fennoscandia as imaged by the BEAR array. Contributed paper presented at the joint European Geosciences Union – American Geophysical Union meeting, Nice, France, April 6–11, 2003.

Kusky, T.M. 1989. Accretion of the Archean Slave province. Geology, **17**: 63–67.

Kusky, T.M. 1990. Evidence for Archean ocean opening and closing in the southern Slave Province. Tectonics, **9**: 1533–1563.

Ledo, J., and Jones, A.G. 2001. Regional electrical resistivity structure of the southern Canadian Cordillera and its physical interpretation. Journal of Geophysical Research, **106**: 30 775 – 30 769.

Ledo, J., and Jones, A.G. 2005. Temperature of the upper mantle beneath the Intermontane Belt, northern Canadian Cordillera, determined from combining mineral composition, electrical conductivity laboratory studies and magnetotelluric field observations. Earth and Planetary Science Letters, **236**: 258–268.

Ledo, J., Jones, A.G., and Ferguson, I.J. 2002. Electromagnetic images of a strike-slip fault: the Tintina fault-northern Canadian Cordillera. Geophysical Research Letters, **89**: 1530–1533.

Ledo, J., Jones, A.G., Ferguson, I.J., and Wolynec, L. 2004. Lithospheric structure of the Yukon, Northern Canadian Cordillera, obtained from magnetotelluric data. Journal of Geophysical Research, **109**: B04410-1 – B04410-15, doi: 10.1029/2003JB002516.

Lewis, T.J., and Hyndman, R.D. 1998. Heat flow transitions along the SNORCLE Transect; asthenospheric flow. *In* SNORCLE Transect and Cordilleran Tectonics Workshop, Simon Fraser University, Burnaby, B.C., 6–8 March 1998. *Compiled by* F. Cook and P. Erdmer. Lithoprobe Secretariat, The University of British Columbia, Vancouver, B.C., Lithoprobe Report No. 64, p. 92.

Lewis, T.J., and Hyndman, R.D. 1999. High heat flow along the SNORCLE Transect. *In* SNORCLE Transect and Cordilleran Tectonics Workshop, University of Calgary, Calgary, Alta., 5–7 March 1999. *Compiled by* F. Cook and P. Erdmer. Lithoprobe Secretariat, The University of British Columbia, Vancouver, B.C., Lithoprobe Report No. 69, pp. 83–84.

Lewis, T.J., and Hyndman, R.D. 2001. High heat flow and high crustal temperatures along the SNORCLE Transect. *In* SNORCLE Transect and Cordilleran Tectonics Workshop Meeting, Sidney, B.C., 25–27 Feb. 2001. *Edited by* F.A. Cook and P. Erdmer. Lithoprobe Secretariat, The University of British Columbia, Vancouver, B.C., Lithoprobe Report No. 79, pp. 28–29.

Lewis, T.J., Hyndman, R., and Fluck, X. 2003. Heat flow, heat generation, and crustal temperatures in the northern Canadian Cordillera: Thermal controls on tectonics. Journal of Geophysical Research, **108**: 2316, doi: 10.1029/2002JB002090.

Majorowicz, J.A. 1996. Anomalous heat flow regime in the western margin of the North, American craton. Journal of Geodynamics, **21**: 123–140.

McNeice, G., and Jones, A.G. 1998. Magnetotellurics in the frozen north: measurements on lake ice. Contributed paper at 14th EM Induction Workshop, Sinaia, Romania, 16–23 August, 1998

Mibe, K., Fujii, T., and Yasuda, A. 1998. Connectivity of aqueous fluid in the Earth's upper mantle. Geophysical Research Letters, **25**: 1233–1236.

Narod, B.B, and Bennest J.R. 1990. Ring-core fluxgate magnetometers for use as observatory variometers. Physics of the Earth and Planetary Interiors, **59:** 23–28.

Niblett, E.R., and Sayn-Wittgenstein, C. 1960. Variation of the electrical conductivity with depth by the magnetotelluric method. Geophysics, **25**: 998–1008.

Ogawa, Y., Jones, A.G., Unsworth, M.J., Booker, J.R., Lu, X., Craven, J., Roberts, B., Parmelee, J., and Farquharson, C. 1996. Deep electrical conductivity structures of the Appalachian Orogen in the southeastern US. Geophysical Research Letters, **23**: 1597–1600.

Pearson, N.J., Griffin, W.L., Doyle, B.J., O'Reilly, S.Y., Van Achterbergh, E., and Kivi, K. 1999. Xenoliths from kimberlite pipes of the Lac de Gras area, Slave craton, Canada. *In* Proceedings of the 7th international Kimberlite conference. *Edited by* J.J. Gurney and P.H. Nixon. Red Roof Design, Cape Town, South Africa, Vol. 2, pp. 644–658.

Petitt, R.A., Jr., Chave, A.D., Filloux, J.H., and Moeller, H.H. 1994. Electromagnetic field instrument for the continental shelf. Sea Technology, **35**: 10–13.

Pilkington, M., Miles, W.F., Ross, G.M., and Roest, W.R. 2000. Potential-field signatures of buried Precambrian basement in the Western Canada Sedimentary Basin, Canadian Journal of Earth Sciences, **37**: 1453–1471.

Ritts, B.D., and Grotzinger, J.P. 1994. Depositional facies and detrital composition of the Paleoproterozoic Et-Then Group, N.W.T., Canada: sedimentary response to intracratonic indentation. Canadian Journal of Earth Sciences, **31**: 1763–1778.

Rodi, W., and Mackie, R.L. 2001. Nonlinear conjugate gradients algorithm for 2-D magnetotelluric inversion. Geophysics, **66**: 174–187.

Simpson, F. 2001. Resistance to mantle flow inferred from the electromagnetic strike of the Australian upper mantle. Nature (London), **412**: 632–634.

© 2005 NRC Canada

Snyder, D.B., Clowes, R.M., Cook, F.A., Erdemer, P., Evenchik, C.A., van der Velden, A.J., and Hall, K.W. 2002. Proterozoic prism arrests suspect terranes: insights into the ancient cordilleran margin from seismic reflection data. Geological Society of America Today, 4–10 October 2002.

Stanley, W.D., Labson, V.F., Nokleberg, W.J., Csejtey, B., and Fisher, M.A. 1990. The Denali fault system and Alaska Range of Alaska: evidence for underplated Mesozoic flysch from magnetotelluric surveys. Geological Society of America Bulletin, **102**: 160–173.

Villeneuve, M.E., Theriault, R.J., and Ross, G.M. 1991. U–Pb ages and Sm–Nd signature of two subsurface granites from the Fort Simpson magnetic high, northwest Canada. Canadian Journal of Earth Sciences, **28**: 1003–1008.

Vozoff, K. (*Editor*). 1986. Magnetotelluric methods. Society of Exploration Geophysicists, Tulsa, Okla., Reprint Series No. 5, ISBN 0-931830-36-2.

Wannamaker, P.E., Chave, A.D., Booker, J.R., Jones, A.G., Filloux, J.H., Ogawa, Y., Unsworth, M., and Evans, R. 1996. Sutures and deep physical state of the SE U.S. Atlantic margin: The Southern Appalachians magnetotelluric experiment. EOS, **77**: 329–333.

Wennberg, G. 2003. Magnetotelluric response of the Northern Cordillera: Interpretation of the lithospheric structure of the SNORCLE Transect, Corridor 2, Line 2a and Connector Line. M.Sc. thesis, University of Manitoba, Winnipeg, Man.

Wennberg, G., Ferguson, I.J., Ledo, J., and Jones, A.G. 2002. Modeling and interpretation of magnetotelluric data: Watson Lake to Stewart (line2A) and Johnsons's Crossing to Watson lake. *In* SNORCLE Transect and Cordilleran Tectonics Workshop, Sidney, B.C., 21–24 Feb. 2002. Lithoprobe Secretariat, The University of British Columbia, Vancouver, B.C., Lithoprobe Report No. 82, p. 145.

Wessel, P., and Smith, W.H.F. 1991. Free software help map and display data. EOS, **72**: 441.

Wolynec, L.L. 2000. LITHOPROBE magnetotelluric crustal study of the Carcross Area, Yukon Territory, B.Sc. (Honours) thesis, University of Manitoba, Winnipeg, Man.

Wu, X. 2001. Determination of near-surface, crustal, and lithospheric structure in the Canadian Precambrian Shield using the time-domain electromagnetic and magnetotelluric methods, Ph.D. thesis, University of Manitoba, Winnipeg, Man.

Wu, X., Ferguson, I.J., and Jones, A.G. 2002. Magnetotelluric response and geoelectric structure of the Great Slave Lake Shear Zone. Earth and Planetary Science Letters, **196**: 35–50.

Wu, X., Ferguson, I.J., and Jones, A.G. 2005. Geoelectric structure of the Proterozoic Wopmay Orogen and adjacent terranes, Northwest Territories, Canada. Canadian Journal of Earth Sciences, **42**: this issue.

Xu, Y., Shankland, T.J., and Poe, B.T. 2000. Laboratory-based electrical conductivity of the Earth's mantle. Journal of Geophysical Research, **105**: 27 865 – 27 875.

© 2005 NRC Canada